THE
PHYSICAL REVIEW

A journal of experimental and theoretical physics established by E. L. Nichols in 1893

SECOND SERIES, Vol. 133, No. 3A 3 FEBRUARY 1964

Frequency Shifts in Spin-Exchange Optical Pumping Experiments*

L. C. BALLING, R. J. HANSON,† AND F. M. PIPKIN‡
Lyman Laboratory of Physics, Harvard University, Cambridge, Massachusetts
(Received 21 June 1963)

A theory is derived to predict the density matrices describing two atoms after a spin-exchange collision from the density matrices before the collision and the scattering amplitude for binary collisions. This theory is then applied to a system of quasifree electrons interacting with optically pumped rubidium atoms. For calculating the change in the electron density matrix, the Rb^{85} and Rb^{87} are replaced by a fictitious rubidium isotope with no nuclear spin. Expressions are derived for the change in the light transmission when a radio-frequency field is present at the electron frequency. In addition to the linewidth for the electron signal, the spin-exchange theory predicts a frequency shift the magnitude of which depends upon the two-body scattering amplitude, the rubidium polarization and the rubidium density. Experiments performed to test various aspects of the theory are then reported. The measurements were made on a system of quasifree electrons interacting with rubidium atoms. Measurements of the electron linewidth as a function of temperature indicated that spin-exchange collisions dominated the electron relaxation. The predicted frequency shift was measured by observing the electron resonance frequency first with left circularly polarized light and then with right circularly polarized light. For electrons colliding with rubidium atoms the shift is negative when the rubidium polarization is positive and the ratio of the shift to the linewidth is $\delta\nu_0/\Delta\nu=-0.025\pm0.005$. From the measured values of the shift and the linewidth, a value is derived for the electron–rubidium spin-flip cross section. In one Appendix the replacement of the Rb^{85} and Rb^{87} by the fictitious rubidium isotope with no nuclear spin is justified. In a second Appendix the calculations for the simple electron-rubidium system are generalized and applied to more complicated systems. Results are reported for the change in the density matrix of hydrogen atoms when they collide with polarized electrons, the change in the density matrix of Rb^{87} atoms when they collide with polarized electrons, and the change in the density matrix of hydrogen atoms when they collide with hydrogen atoms.

INTRODUCTION

ONE of the newer forms of high-precision radio-frequency spectroscopy is spin-exchange optical pumping. In this type of experiment an alkali-metal vapor such as rubidium is polarized by the absorption of circularly polarized optical resonance radiation and the polarization is monitored by observing the transmission of optical resonance radiation through the flask containing the alkali metal. Another species of atom such as hydrogen is polarized by spin-exchange collisions with the oriented rubidium. If a radio-frequency field is adjusted so as to depolarize the hydrogen, the rubidium will be depolarized through spin-exchange collisions and the transmission of light by the absorption flask will decrease. In this manner the radio-frequency spectrum of hydrogen can be measured. This technique can be refined so as to make possible very precise measurements. The spin-exchange optical pumping method has been used to measure the gyromagnetic ratio of quasifree electrons,[1] the hyperfine splittings of hydrogen, deuterium, and tritium,[2,3] the hyperfine splittings[4–7] of the nitrogen isotopes, the hyperfine splitting of phosphorus,[8] and the gyromagnetic ratio

* Research supported in part by the Sloan Foundation and in part by the National Science Foundation.
† National Science Foundation Faculty Fellow on leave at Harvard University at the time this research was undertaken. Present address: Grinnell College, Grinnell, Iowa.
‡ Alfred P. Sloan Research Fellow, 1961–1963.

[1] H. G. Dehmelt, Phys. Rev. **109**, 381 (1958).
[2] L. W. Anderson, F. M. Pipkin, and J. C. Baird, Jr., Phys. Rev. **120**, 1279 (1960); **121**, 1874 (1961); **121**, 1962 (1961).
[3] F. M. Pipkin and R. H. Lambert, Phys. Rev. **127**, 787 (1962).
[4] L. W. Anderson, F. M. Pipkin, and J. C. Baird, Jr., Phys. Rev. **116**, 87 (1959).
[5] W. W. Holloway, Jr., and E. Lüscher, Nuovo Cimento **18**, 1926 (1960).
[6] W. W. Holloway, Jr., E. Lüscher, and R. Novick, Phys. Rev. **126**, 2109 (1962).
[7] R. H. Lambert and F. M. Pipkin, Phys. Rev. **129**, 1233 (1963).
[8] R. H. Lambert and F. M. Pipkin, Phys. Rev. **128**, 198 (1962); **129**, 2836 (1963).

of silver.[9] Recently there was reported an analogous experiment in which the hydrogen maser was used to determine by a spin-exchange technique the hyperfine splitting of atomic deuterium.[10] Spin exchange may also be a useful technique for studying the radio-frequency spectra of ions.[11]

So far there have been no extensive investigations of the magnitudes of spin-exchange cross sections nor of the possible frequency shifts due to spin-exchange collisions.[12] In the general theory of collision broadening it is shown that a scattering process which gives a linewidth will also in general give a frequency shift.[13] The linewidth and the frequency shift are related to the scattering amplitude for two-body collisions. On this basis one would expect frequency shifts from spin-exchange collisions.[14]

Spin-exchange collisions give one of the few electron-nuclear relaxation mechanisms where the complete interaction Hamiltonian is known and where the problem is simple enough that an exact solution for the rate of change of the density matrix describing the two colliding species should be possible. Previous to the work reported in this paper most of the calculations in the literature attempted to deal only with the diagonal elements of the density matrix.[1,4] Wittke and Dicke[15,16] took a simple model for hydrogen-hydrogen spin-exchange collisions and calculated part of the nuclear relaxation. They used a form of exchange operator to calculate the change in the density matrix rather than the exact scattering matrix which describes hydrogen-hydrogen collisions.

This paper reports an investigation of the systematics of spin-exchange collisions. In the first part a simple theory is developed to describe the signals in spin-exchange optical pumping experiments. Calculations are made for a system consisting of an optically pumped atom with a $^2S_{1/2}$ electronic ground state and no nuclear spin (called rubidium) interacting through spin-exchange collisions with a second system with electronic spin $\frac{1}{2}$ and no nuclear spin (called the electron). It is assumed that the scattering amplitude (phase shifts) for rubidium-electron collisions is known and the change in the density matrix describing the two atoms due to spin-exchange collisions is calculated. A calculation is then made of the change in the amount of light transmitted by the bulb when a radio-frequency field is applied so as to disorient the electrons. These calculations show that the electron resonance line has a Lorentzian shape the width of which depends upon the number of spin-exchange collisions per second and the center of which will in general be shifted by an amount which depends upon the spin-exchange collision amplitude, the rubidium polarization, and the number of spin-exchange collisions per second. In an Appendix the calculations are generalized so as to allow each of the colliding species to have a nuclear spin. The formalism is essentially the same as that employed for the two spin $\frac{1}{2}$ systems. Results are reported for rubidium and electrons, hydrogen and electrons, and hydrogen and hydrogen. The last part of the paper describes measurements made on a system of quasifree electrons colliding with optically pumped rubidium atoms. The form of the optical pumping signals is shown to be well represented by the theory. In order to determine the spin-exchange cross section, measurements were made of the electron resonance linewidth and the frequency shift as a function of rubidium density. From the measured shift and linewidth, a value is derived for the spin-exchange cross section.

THEORY

A. The Effect of Spin-Exchange Collisions

Figure 1 shows a schematic representation of the absorption bulb containing the free electrons and the

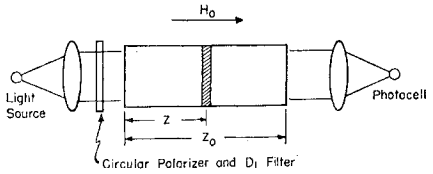

FIG. 1. Schematic representation of an idealized optical pumping system.

[9] G. S. Hayne and H. G. Robinson, Bull. Am. Phys. Soc. **5**, 411 (1960).

[10] S. B. Crampton, D. Kleppner, and H. C. Robinson, Bull. Am. Phys. Soc. **8**, 351 (1963).

[11] H. G. Dehmelt, Bull. Am. Phys. Soc. **8**, 23 (1963).

[12] Some references in which spin-exchange cross sections have been measured or estimated are the following:

H–H	E. M. Purcell and G. B. Field, Astrophys. J. **124**, 542 (1956).
H–H	A. Dalgarno, Proc. Roy. Soc. (London) **A262**, 132 (1961).
H–H	J. P. Wittke and R. H. Dicke, Phys. Rev. **103**, 620 (1956).
H–H	A. F. Hildebrandt, F. B. Booth, and C. A. Barth, J. Chem. Phys. **31**, 273 (1959).
H–H	R. M. Mazo, J. Chem. Phys. **34**, 169 (1961).
e–H	P. Burke and H. M. Schey, Phys. Rev. **126**, 163 (1962).
e–Na	H. G. Dehmelt, Phys. Rev. **109**, 381 (1958).
K–Na	P. Franken, R. Sands, and J. Hobart, Phys. Rev. Letters **1**, 54 (1958).
e–K	P. Franken, R. Sands, and J. Hobart, Phys. Rev. Letters **1**, 54 (1958).
Na–Rb	R. Novick and H. E. Peters, Phys. Rev. Letters **1**, 54 (1958).
Rb–N	L. W. Anderson, F. M. Pipkin, and J. C. Baird, Jr., Phys. Rev. **116**, 87 (1959).

[13] See, for example, M. Baranger, in *Atomic and Molecular Processes*, edited by D. R. Bates (Academic Press Inc., New York, 1962), pp. 493–546.

[14] During the course of this work we learned that a frequency shift similar to that reported in this paper was observed by P. Franken, and J. Hobart [J. Hobart, thesis, University of Michigan, 1962 (unpublished)]. Also a paper was published [R. R. Lewis, Phys. Rev. **130**, 666 (1963)] in which an explanation was proposed for the shift observed by Hobart. Our formulas for the linewidth and line shift do not agree with those given by Lewis.

[15] J. P. Wittke and R. H. Dicke, Phys. Rev. **103**, 620 (1956).

[16] J. P. Wittke, thesis, Princeton University, 1955 (unpublished).

rubidium vapor. To describe the system we shall use a Cartesian coordinate system the origin of which is at the center of the front face and the z axis of which coincides with the axis of the cylindrical absorption flask. The external magnetic field H_0 and the light beam are assumed to be parallel to the z axis. It will be assumed that left circularly polarized (positive helicity) rubidium resonance radiation from the $(5P_{1/2} \rightarrow 5S_{1/2})$ transition is incident on the bulb and that the rubidium and the electrons are immersed in a buffer gas the density of which is such that there is complete reorientation in the optically excited state of the rubidium.[17] It will be assumed that there is no relaxation of the orientation at the walls of the absorption bulb. By the signals we shall mean the change in the amount of light transmitted by the cell. In order to calculate the signals, we must consider the behavior of the electron and rubidium spin systems under the influence of the pumping light and the radio-frequency field and how the two systems are coupled through spin exchange. A suitable way to characterize the electron-rubidium spin system quantum mechanically is by electron and rubidium spin-space density matrices. First, we will calculate the change in the two density matrices due to spin-exchange collisions; second, we will calculate the behavior of the electron density matrix under the influence of the radio-frequency field; and finally, we will calculate the change in the amount of light transmitted by the absorption cell due to the presence of the radio-frequency field.

For these calculations we will assume that the rubidium atoms have no nuclear spin and work with a fictitious 2×2 density matrix for the rubidium rather than the full density matrix which describes the two isotopes. This simplifies the algebra and gives essentially the same result as that obtained using the complete density matrices. This approximation is justified in Appendix A. The spin-space density matrix for the electrons can be written in the form

$$\rho(e)=\begin{pmatrix}\rho_{11}(e) & \rho_{12}(e)\\ \rho_{21}(e) & \rho_{22}(e)\end{pmatrix} \tag{1}$$

and that for the rubidium

$$\rho(R)=\begin{pmatrix}\rho_{11}(R) & 0\\ 0 & \rho_{22}(R)\end{pmatrix}. \tag{2}$$

Here 1 denotes the $+\frac{1}{2}$ state and 2, the $-\frac{1}{2}$ state. It has been assumed that the off-diagonal elements of the rubidium density matrix are zero. In general, the two density matrices will be a function of the position in the bulb. For our restricted assumption of no relaxation at the walls of the cell they will be a function only of z. This functional dependence arises from the change in the spectral distribution and intensity of the incident light as it passes through the bulb. For our initial discussion of the spin-exchange collisions we will consider only one region in the bulb and the dependence of the density matrices on position will be suppressed. We will ignore correlations between the rubidium-electron systems and assume that the density matrix for the electron-rubidium system is just the direct product of the electron and rubidium density matrices. That is, we write

$$\rho(e,R)=\rho(e)\times\rho(R)$$
$$=\begin{bmatrix}\rho_{11}(e)\rho_{11}(R) & 0 & \rho_{12}(e)\rho_{11}(R) & 0\\ 0 & \rho_{11}(e)\rho_{22}(R) & 0 & \rho_{12}(e)\rho_{22}(R)\\ \rho_{21}(e)\rho_{11}(R) & 0 & \rho_{22}(e)\rho_{11}(R) & 0\\ 0 & \rho_{21}(e)\rho_{22}(R) & 0 & \rho_{22}(e)\rho_{22}(R)\end{bmatrix}. \tag{3}$$

The following procedure will be employed to calculate the effect of collisions between the electrons and rubidium atoms upon the density matrix. We will first write the density matrix for the electron-rubidium system which includes the momentum states. We will then use the scattering matrix for rubidium-electron collisions to calculate the density matrix after a collision from that before a collision. We obtain the spin-space density matrix by tracing over the momentum states and finally the density matrix for either the electron or rubidium by tracing over the spin coordinates corresponding to the irrelevant particle. In writing down the S matrix and the momentum states we shall for purposes of normalization use a cubic box one side of which has length L. The scattering of the electron by the rubidium will be described in the center-of-mass system using coordinates of the electron relative to the rubidium.[18] The incoming wave for the electron-rubidium scattering problem can be written in the form

$$(1/L^{3/2})\exp(i\mathbf{k}_0\cdot\mathbf{r})\,|s_0\rangle, \tag{4}$$

where $|s_0\rangle$ is the initial electron-rubidium spin state, and the normalization is such that we have one electron in the box. For distinguishable particles the scattered wave will have the form

$$\psi(r,\mathbf{k},s)=(1/L^{3/2})[\exp(i\mathbf{k}_0\cdot\mathbf{r})\,|s_0\rangle + (e^{ikr}/r)M_{ss_0}(\mathbf{k};\mathbf{k}_0)\,|s_0\rangle], \tag{5}$$

where $M_{ss_0}(\mathbf{k};\mathbf{k}_0)$ is a function of the angle between $\mathbf{k}$ and $\mathbf{k}_0$ and is in general a matrix in spin space which allows for the possibility of changes in spin states during a collision. For our calculations we will assume that $M_{ss_0}(\mathbf{k};\mathbf{k}_0)$ can be written in the form

$$M_{ss_0}(\mathbf{k};\mathbf{k}_0)=a(\mathbf{k},\mathbf{k}_0)+b(\mathbf{k},\mathbf{k}_0)\boldsymbol{\sigma}_R\cdot\boldsymbol{\sigma}_e. \tag{6}$$

This form of the M matrix results if one assumes that there is no spin-orbit coupling and that the scattering can be described in terms of independent phase shifts

[17] W. Franzen and A. G. Emslie, Phys. Rev. 108, 1453 (1957).

[18] A. Messiah, *Quantum Mechanics* (North-Holland Publishing Company, Amsterdam, 1962), Vol. II, pp. 801, 872.

in the singlet and triplet states. With these assumptions we can write

$$M=f_3(\theta)P_3+f_1(\theta)P_1, \tag{7}$$

where f_3 and f_1 are the triplet and singlet scattering amplitudes and P_3 and P_1 are the projection operators for the triplet and singlet electronic states. In terms of the Pauli spin matrices the projection operators are

$$P_3=\tfrac{1}{4}(3+\boldsymbol{\sigma}_e\cdot\boldsymbol{\sigma}_R), \tag{8}$$

and

$$P_1=\tfrac{1}{4}(1-\boldsymbol{\sigma}_e\cdot\boldsymbol{\sigma}_R). \tag{9}$$

In terms of the triplet and singlet phase shifts, the scattering amplitudes are

$$f_3=\frac{1}{2ik}\sum_{l=0}^{\infty}(2l+1)(e^{2i\delta_l^3}-1)P_l(\cos\theta), \tag{10}$$

and

$$f_1=\frac{1}{2ik}\sum_{l=0}^{\infty}(2l+1)(e^{2i\delta_l^1}-1)P_l(\cos\theta). \tag{11}$$

This model is the one which has been most commonly used in the treatment of spin-exchange collisions.

The complete density matrix operator (including momentum states) for the electron-rubidium system can be written in the form

$$\rho=\sum_{k,s}|\mathbf{k},s\rangle P(\mathbf{k},s)\langle\mathbf{k},s|, \tag{12}$$

where $P(\mathbf{k},s)$ is the probability of finding the state $|\mathbf{k},s\rangle$ in the statistical mixture. If we introduce the S matrix relating the final scattered state to the initial state after an infinitely long time, we can write the density matrix after a collision in the form

$$\rho'=S\rho S^\dagger. \tag{13}$$

In terms of the notation

$$S_{s's}(\mathbf{k}';\mathbf{k})=\langle\mathbf{k}'s'|S|\mathbf{k}s\rangle, \tag{14}$$

the matrix elements of S are related to M by the equation

$$S_{s's}(\mathbf{k}';\mathbf{k})=\delta(\mathbf{k}',\mathbf{k})\delta_{s's}+2\pi i(2\pi\hbar^2/\mu L^3)\delta(E-E')M_{s's}(\mathbf{k}';\mathbf{k}), \tag{15}$$

where E is the energy and μ is the reduced mass. In this same notation the initial density matrix is assumed to be

$$\langle\mathbf{k}'s'|\rho|\mathbf{k}''s''\rangle=\delta(\mathbf{k}',\mathbf{k}^0)\delta(\mathbf{k}'',\mathbf{k}^0)\rho_{s's''}. \tag{16}$$

The spin-state density matrix after a collision is given by taking the trace over the momentum index. That is

$$\rho_{s\bar{s}}'=\sum_{\mathbf{k}}\langle\mathbf{k}s|S\rho S^\dagger|\mathbf{k}\bar{s}\rangle, \tag{17}$$

and

$$\rho_{s\bar{s}}'=\sum_{s's''}\sum_{\mathbf{k},\mathbf{k}',\mathbf{k}''}\langle\mathbf{k}s|S|\mathbf{k}'s'\rangle\times\langle\mathbf{k}'s'|\rho|\mathbf{k}''s''\rangle\langle\mathbf{k}''s''|S^\dagger|\mathbf{k}\bar{s}\rangle. \tag{18}$$

If we insert expressions (15) and (16) into Eq. (18), we obtain

$$\begin{aligned}\rho_{s\bar{s}}'=\sum_{s's''\mathbf{k}}\Big[&\delta(\mathbf{k},\mathbf{k}_0)\delta(\mathbf{k},\mathbf{k}_0)\delta_{ss'}\rho_{s's''}\delta_{s''\bar{s}}\\&+2\pi i\left(\frac{2\pi\hbar^2}{\mu L^3}\right)\delta(E-E_0)M_{ss'}(\mathbf{k}_0;\mathbf{k}_0)\rho_{s's''}\delta_{s''\bar{s}}\delta(\mathbf{k},\mathbf{k}_0)\\&-2\pi i\left(\frac{2\pi\hbar^2}{\mu L^3}\right)\delta(E-E_0)\delta_{ss'}\rho_{s's''}M_{s''\bar{s}}^\dagger(\mathbf{k}_0;\mathbf{k}_0)\delta(\mathbf{k}_0,\mathbf{k})\\&+(2\pi)^2\left(\frac{2\pi\hbar^2}{\mu L^3}\right)^2\delta(E-E_0)\delta(E-E_0)\\&\times M_{ss'}(\mathbf{k};\mathbf{k}_0)\rho_{s's''}M_{s''\bar{s}}^\dagger(\mathbf{k}_0;\mathbf{k})\Big].\end{aligned} \tag{19}$$

When we sum over $\mathbf{k}$ we obtain terms involving $\delta(E_0-E_0)$. In order to interpret this expression we note that in the derivation of Eq. (15) for the S matrix the delta function arose from the time integral

$$\delta(E-E_0)=\lim_{t\to\infty}\frac{1}{2\pi}\int_{-\infty}^{t}e^{-i(E-E_0)t/\hbar}\frac{dt}{\hbar}. \tag{20}$$

In accordance with this equation we can interpret $\delta(E_0-E_0)$ as being $T/2\pi\hbar$, where T is the time elapsed in the scattering process. When evaluating

$$\sum_{\mathbf{k}}\delta(E-E_0)\delta(E-E_0),$$

it is convenient to let $L\to\infty$, so that

$$\sum_{\mathbf{k}}\to L^3\int\frac{d^3k}{(2\pi)^3}=\frac{L^3}{(2\pi)^3}\int\left(\frac{2\mu E}{(\hbar)^2}\right)^{1/2}\frac{\mu}{(\hbar)^2}dEd\Omega. \tag{21}$$

When we perform the final sum over $\mathbf{k}$, we obtain

$$\begin{aligned}\rho_{s\bar{s}}'=\rho_{s\bar{s}}+T\left(\frac{\hbar k}{\mu L^3}\right)\Big[&\frac{2\pi i}{k}\Big(\sum_{s'}M_{ss'}(\mathbf{k}_0;\mathbf{k}_0)\rho_{s'\bar{s}}\\&-\sum_{s''}\rho_{ss''}M_{s''\bar{s}}^\dagger(\mathbf{k}_0;\mathbf{k}_0)\Big)\\&+\int d\Omega\sum_{s's''}M_{ss'}(\mathbf{k};\mathbf{k}_0)\rho_{s's''}M_{s''\bar{s}}^\dagger(\mathbf{k}_0;\mathbf{k})\Big],\end{aligned} \tag{22}$$

where the angular integral is over the angle between $\mathbf{k}$ and $\mathbf{k}_0$ and $|\mathbf{k}|=|\mathbf{k}_0|$. Thus, the time rate change of the electron density matrix due to spin-exchange collisions with the rubidium is

$$\begin{aligned}\frac{d\rho(e)}{dt}=v_{eR}N_R\,\mathrm{Tr}_R\Big[&\frac{2\pi i}{k}[M(\theta=0)\rho(e,R)\\&-\rho(e,R)M^\dagger(\theta=0)]\\&+\int d\Omega M(\cos\theta)\rho(e,R)M^\dagger(\cos\theta)\Big],\end{aligned} \tag{23}$$

where v_{eR} is the relative velocity of the electrons and the rubidium atoms, N_R is the number of rubidium atoms per cm^3, Tr_R stands for the trace over the rubidium spin coordinates, $\rho(e,R)$ is the electron rubidium spin-space density matrix, $M(\cos\theta)$ is an abbreviation for $M_{ss_0}(\mathbf{k};\mathbf{k}_0)$, and θ is the angle between $\mathbf{k}$ and $\mathbf{k}_0$. An analogous expression can be written down for the time rate change of the rubidium density matrix. It is

$$\frac{d\rho(R)}{dt}=v_{eR}N_e\,\mathrm{Tr}_e\Big[\frac{2\pi i}{k}[M(\theta=0)\rho(e,R)-\rho(e,R)M^\dagger(\theta=0)]+\int d\Omega M(\cos\theta)\rho(e,R)M^\dagger(\cos\theta)\Big]. \quad (24)$$

If we assume that the M matrix can be written in the form of Eq. (6) and introduce the spin-flip cross section σ_{SF} and the shift parameter κ where

$$\sigma_{\mathrm{SF}}=\frac{1}{4}\int d\Omega|f_3-f_1|^2=\frac{\pi}{k^2}\sum_{l=0}^{\infty}(2l+1)\sin^2(\delta_l{}^3-\delta_l{}^1), \quad (25)$$

and

$$\kappa=\frac{1}{\sigma_{\mathrm{SF}}}\frac{\pi}{2k^2}\sum_{l=0}^{\infty}(2l+1)\sin 2(\delta_l{}^3-\delta_l{}^1), \quad (26)$$

we can rewrite Eq. (23) in the somewhat simpler form

$$d\rho(e)/dt=\tfrac{1}{4}v_{eR}N_R\sigma_{\mathrm{SF}}\,\mathrm{Tr}_R[-3\rho(e,R)+(1+2i\kappa)(\boldsymbol{\sigma}_e\cdot\boldsymbol{\sigma}_R)\rho(e,R)+(1-2i\kappa)\rho(e,R)(\boldsymbol{\sigma}_e\cdot\boldsymbol{\sigma}_R)+(\boldsymbol{\sigma}_e\cdot\boldsymbol{\sigma}_R)\rho(e,R)(\boldsymbol{\sigma}_e\cdot\boldsymbol{\sigma}_R)]. \quad (27)$$

This form is the most convenient for calculational purposes. For our simple electron-rubidium system

$$\boldsymbol{\sigma}_e\cdot\boldsymbol{\sigma}_R=\begin{pmatrix}1&0&0&0\\0&-1&2&0\\0&2&-1&0\\0&0&0&1\end{pmatrix}. \quad (28)$$

The explicit equations for the time rate change of the electron density matrix are

$$d\rho_{11}(e)/dt=v_{eR}N_R\sigma_{\mathrm{SF}}[\rho_{22}(e)\rho_{11}(R)-\rho_{11}(e)\rho_{22}(R)]; \quad (29)$$

$$d\rho_{22}(e)/dt=v_{eR}N_R\sigma_{\mathrm{SF}}[\rho_{11}(e)\rho_{22}(R)-\rho_{22}(e)\rho_{11}(R)]; \quad (30)$$

$$d\rho_{12}(e)/dt=v_{eR}N_R\sigma_{\mathrm{SF}}[-\rho_{12}(e)+i\kappa(\rho_{11}(R)-\rho_{22}(R))\rho_{12}(e)]; \quad (31)$$

$$d\rho_{21}(e)/dt=v_{eR}N_R\sigma_{\mathrm{SF}}[-\rho_{21}(e)-i\kappa(\rho_{11}(R)-\rho_{22}(R))\rho_{21}(e)]. \quad (32)$$

If we introduce the rubidium and electron polarizations

$$P(e)=\rho_{11}(e)-\rho_{22}(e), \quad (33)$$

$$P(R)=\rho_{11}(R)-\rho_{22}(R), \quad (34)$$

and the spin-exchange relaxation time for the electrons

$$1/T_{ee}=v_{eR}N_R\sigma_{\mathrm{SF}}, \quad (35)$$

we can rewrite Eqs. (29) through (32) in the somewhat simpler form

$$\frac{d\rho(e)}{dt}=\begin{pmatrix}\dfrac{P(R)-P(e)}{2T_{ee}} & -\dfrac{1-i\kappa P(R)}{T_{ee}}\rho_{12}(e)\\ -\dfrac{1+i\kappa P(R)}{T_{ee}}\rho_{21}(e) & \dfrac{P(e)-P(R)}{2T_{ee}}\end{pmatrix}. \quad (36)$$

The presence of the imaginary term in Eq. (36) indicates that the spin-exchange collisions have the effect of rotating the electron spin, and thus they will lead to a change in the electron resonance frequency. In a similar fashion for the rubidium we obtain

$$\frac{d\rho(R)}{dt}=\begin{pmatrix}\dfrac{P(e)-P(R)}{2T_{eR}} & 0\\ 0 & \dfrac{P(R)-P(e)}{2T_{eR}}\end{pmatrix}, \quad (37)$$

where

$$1/T_{eR}=v_{eR}N_e\sigma_{\mathrm{SF}}. \quad (38)$$

Here N_e is the number of electrons per cm^3.

In Appendix B, this method is used to calculate the change in the density matrix for hydrogen colliding with polarized electrons, rubidium colliding with polarized electrons, and hydrogen with hydrogen. All other relaxation mechanisms can be introduced through the phenomenological equations

$$\frac{d\rho(e)}{dt}=\begin{pmatrix}\dfrac{\frac{1}{2}-\rho_{11}(e)}{T_{1e}} & -\dfrac{\rho_{12}(e)}{T_{2e}}\\ -\dfrac{\rho_{21}(e)}{T_{2e}} & \dfrac{\frac{1}{2}-\rho_{22}(e)}{T_{1e}}\end{pmatrix}, \quad (39)$$

$$\frac{d\rho(R)}{dt}=\begin{pmatrix}\dfrac{\frac{1}{2}-\rho_{11}(R)}{T_{1R}} & -\dfrac{\rho_{12}(R)}{T_{2R}}\\ -\dfrac{\rho_{21}(R)}{T_{2R}} & \dfrac{\frac{1}{2}-\rho_{22}(R)}{T_{1R}}\end{pmatrix}. \quad (40)$$

B. Effect of the Radio-Frequency Field

We will now consider the effect of a radio-frequency field upon the electron density matrix. In the presence of a static magnetic field H_0 along the direction of the light beam (z axis) and a radio-frequency field $2H_1\cos\omega t$ in the direction of the x axis, the Hamiltonian

for the electrons will be

$$\mathcal{H}=-g_J\mu_0 H_0 J_z-2g_J\mu_0 H_1 J_x\cos\omega t. \tag{41}$$

In terms of the Pauli spin matrices, $\mathcal{H}$ has the form

$$\mathcal{H}=\tfrac{1}{2}\hbar\omega_0\sigma_z+\hbar\omega_1\sigma_x\cos\omega t, \tag{42}$$

where

$$\omega_0=-g_J\mu_0 H_0/\hbar; \tag{43}$$

$$\omega_1=-g_J\mu_0 H_1/\hbar. \tag{44}$$

The equations of motion of the electron density operator due to this Hamiltonian are

$$i\hbar\dot{\rho}(e)=\mathcal{H}\rho(e)-\rho(e)\mathcal{H}. \tag{45}$$

These equations are simplified if we transform to a rotating coordinate system by means of the transformation

$$\tilde{\rho}(e)=e^{i\sigma_z\omega t/2}\rho(e)e^{-i\sigma_z\omega t/2}. \tag{46}$$

In this coordinate system,

$$i\hbar d\tilde{\rho}(e)/dt=[e^{i\sigma_z\omega t/2}\mathcal{H}e^{-i\sigma_z\omega t/2},\tilde{\rho}(e)]-\tfrac{1}{2}\hbar\omega[\sigma_z,\tilde{\rho}(e)]. \tag{47}$$

If we ignore the counter rotating components of the magnetic field, we obtain for the time rate change of the density matrix elements the equations

$$\begin{aligned}
&d\tilde{\rho}_{11}(e)/dt=-\tfrac{1}{2}i\omega_1(\tilde{\rho}_{21}(e)-\tilde{\rho}_{12}(e));\\
&d\tilde{\rho}_{22}(e)/dt=-\tfrac{1}{2}i\omega_1(\tilde{\rho}_{12}(e)-\tilde{\rho}_{21}(e));\\
&d\tilde{\rho}_{12}(e)/dt=-i(\omega_0-\omega)\tilde{\rho}_{12}(e)-\tfrac{1}{2}i\omega_1(\tilde{\rho}_{22}(e)-\tilde{\rho}_{11}(e));\\
&d\tilde{\rho}_{21}(e)/dt=i(\omega_0-\omega)\tilde{\rho}_{21}(e)-\tfrac{1}{2}i\omega_1(\tilde{\rho}_{11}(e)-\tilde{\rho}_{22}(e)).
\end{aligned} \tag{48}$$

Combining the spin-exchange equations and the other relaxation equations with Eq. (48), we obtain in the rotating coordinate system the equations

$$\begin{aligned}
&\frac{d\tilde{\rho}_{11}(e)}{dt}=\frac{P(R)-P(e)}{2T_{ee}}+\frac{\tfrac{1}{2}-\tilde{\rho}_{11}(e)}{T_{1e}}-\frac{i\omega_1}{2}(\tilde{\rho}_{21}(e)-\tilde{\rho}_{12}(e));\\
&\frac{d\tilde{\rho}_{22}(e)}{dt}=\frac{P(e)-P(R)}{2T_{ee}}+\frac{\tfrac{1}{2}-\tilde{\rho}_{22}(e)}{T_{1e}}-\frac{i\omega_1}{2}(\tilde{\rho}_{12}(e)-\tilde{\rho}_{21}(e));\\
&d\tilde{\rho}_{12}(e)/dt=-(T_{ee}^{-1}+T_{2e}^{-1})\tilde{\rho}_{12}(e)-i(\omega_0-\delta\omega_0-\omega)\tilde{\rho}_{12}-\tfrac{1}{2}i\omega_1(\tilde{\rho}_{22}(e)-\tilde{\rho}_{11}(e));\\
&d\tilde{\rho}_{21}(e)/dt=-(T_{ee}^{-1}+T_{2e}^{-1})\tilde{\rho}_{21}(e)+i(\omega_0-\delta\omega_0-\omega)\tilde{\rho}_{21}-\tfrac{1}{2}i\omega_1(\tilde{\rho}_{11}(e)-\tilde{\rho}_{22}(e)),
\end{aligned} \tag{49}$$

where

$$\delta\omega_0=2\pi\delta\nu_0=P(R)\kappa/T_{ee}. \tag{50}$$

These equations are a form of the Bloch equations and they can be solved in a similar fashion.[19,20] If we introduce the abbreviation

$$\frac{1}{\tau_2}=\frac{1}{T_{2e}}+\frac{1}{T_{ee}}, \tag{51}$$

and solve for the equilibrium case when

$$d\tilde{\rho}_{11}/dt=d\tilde{\rho}_{22}/dt=d\tilde{\rho}_{12}/dt=d\tilde{\rho}_{21}/dt=0,$$

we obtain the equations

$$\tilde{\rho}_{12}(e)=(\tilde{\rho}_{21}(e))^*=\tfrac{1}{2}\omega_1\tau_2\left[\frac{i+\tau_2(\omega_0-\delta\omega_0-\omega)}{1+(\tau_2)^2(\omega_0-\delta\omega_0-\omega)^2}\right]P(e), \tag{52}$$

$$\frac{P(R)}{T_{ee}}=\left[\frac{1}{T_{1e}}+\frac{1}{T_{ee}}+\frac{\omega_1^2\tau_2}{1+(\tau_2)^2(\omega_0-\delta\omega_0-\omega)^2}\right]P(e). \tag{53}$$

C. Calculation of the Signals

We now wish to include the effects of the pumping light and to complete the calculation of the electron signals. The light absorption cross section for the rubidium can be written in the form[21]

$$\sigma(\nu)=\sigma_0\exp\{-4\ln 2[(\nu-\nu_0)/\Delta\nu_D]^2\}, \tag{54}$$

where ν is the frequency and $\Delta\nu_D$ is the full width at half-maximum of the Doppler broadened absorption line,

$$\Delta\nu_D=2(2\ln 2)^{1/2}(\nu_0/c)(RT/M)^{1/2}. \tag{55}$$

Here c is the velocity of light, R the universal gas constant, and M the molecular weight of rubidium. The constant σ_0 can be estimated from the dispersion theory expression for the total absorption cross section for circularly polarized light,

$$\int_0^\infty\sigma(\nu)d\nu=\tfrac{1}{3}\pi c r_0, \tag{56}$$

where r_0 is the classical radius of the electron and $\frac{1}{3}$ is the oscillator strength for circularly polarized $D_1(5P_{1/2}\rightarrow 5S_{1/2})$ resonance radiation. This expression for the total cross section is the average of the cross sections of the various magnetic substates of the ground state. It will be assumed that the light intensity per unit frequency range per second of circularly polarized D_1 photons is

$$I(\nu,0)=I_0\exp\{-4\ln 2[(\nu-\nu_0)/\alpha\Delta\nu_D]^2\}. \tag{57}$$

This assumes the light source has a Doppler spectral distribution whose width is $\alpha\Delta\nu_D$. The constant I_0 is given by

$$I_0=\left(\frac{2(\ln 2)^{1/2}}{\alpha\pi^{1/2}\Delta\nu_D}\right)\int_0^\infty I(\nu,0)d\nu. \tag{58}$$

[19] H. C. Torrey, Phys. Rev. **104**, 563 (1956).

[20] A. Abragam, *The Principles of Nuclear Resonance* (Oxford University Press, Oxford, England, 1961), p. 44.

[21] A. C. G. Mitchell and M. W. Zemansky, *Resonance Radiation and Excited Atoms* (Cambridge University Press, Cambridge, 1934), Chap. III, pp. 92–152.

The absorption of light by the rubidium atoms makes the light intensity, $I(\nu,z)$, a function of z, the distance from the front of the absorption bulb. In the presence of the light source the equations of motion of the diagonal elements of the rubidium density matrix are

$$\dot{\rho}_{11}(R,z)=\left(\int_0^\infty I(\nu,z)\sigma(\nu)d\nu\right)\rho_{22}(R,z)+\frac{\frac{1}{2}-\rho_{11}(R,z)}{T_{1R}}+\frac{P(e,z)-P(R,z)}{2T_{eR}}; \quad (59)$$

$$\dot{\rho}_{22}(R,z)=-\left(\int_0^\infty I(\nu,z)\sigma(\nu)d\nu\right)\rho_{22}(R,z)+\frac{\frac{1}{2}-\rho_{22}(R,z)}{T_{1R}}-\frac{P(e,z)-P(R,z)}{2T_{eR}}; \quad (60)$$

and for the variation in light intensity we have the equation

$$\partial I(\nu,z)/\partial z=-2\sigma(\nu)I(\nu,z)N_R\rho_{22}(R,z). \quad (61)$$

Equation (61) has the solution

$$I(\nu,z)=I(\nu,0)\exp\left[-2\int_0^z N_R\sigma(\nu)\rho_{22}(R,\xi)d\xi\right]. \quad (62)$$

If Eqs. (59) and (60) are averaged over z they can be rewritten in the form

$$\langle\dot{\rho}_{11}(R)\rangle=\left(\frac{1}{2N_Rz_0}\right)\int_0^\infty I(\nu,0)(1-e^{-2N_R\sigma(\nu)z_0\langle\rho_{22}(R)\rangle})d\nu+\frac{\frac{1}{2}-\langle\rho_{11}(R)\rangle}{T_{1R}}+\frac{\langle P(e)\rangle-\langle P(R)\rangle}{2T_{eR}}; \quad (63)$$

$$\langle\dot{\rho}_{22}(R)\rangle=-\frac{1}{2}\left(\frac{1}{N_Rz_0}\right)\int_0^\infty I(\nu,0)(1-e^{-2N_R\sigma(\nu)z_0\langle\rho_{22}(R)\rangle})d\nu+\frac{\frac{1}{2}-\langle\rho_{22}(R)\rangle}{T_{1R}}+\frac{\langle P(R)\rangle-\langle P(e)\rangle}{2T_{eR}}, \quad (64)$$

where z_0 is the length of the absorption bulb and $\langle\ \rangle$ denotes the average over z.

$$\langle A\rangle=\frac{1}{z_0}\int_0^{z_0}A(z)dz. \quad (65)$$

If we introduce the auxiliary functions[21]

$$s=2N_R\sigma_0z_0\langle\rho_{22}(R)\rangle=N_R\sigma_0z_0[1-\langle P(R)\rangle], \quad (66)$$

$$A_\alpha(s)=\int_{-\infty}^{+\infty}e^{-(\omega/\alpha)^2}[1-\exp(-se^{-\omega^2})]d\omega\Big/\int_{-\infty}^{+\infty}e^{-(\omega/\alpha)^2}d\omega, \quad (67)$$

we can combine (63) and (64) into the following equation for the rubidium polarization.

$$\frac{d}{dt}\langle P(R)\rangle=\frac{A_\alpha(s)}{N_Rz_0}\int_0^\infty I(\nu,0)d\nu-\left(\frac{1}{T_{1R}}+\frac{1}{T_{eR}}\right)\langle P(R)\rangle+\frac{1}{T_{eR}}\langle P(e)\rangle. \quad (68)$$

A short examination shows that, if the magnetic field is homogeneous, Eq. (53) can also be averaged over z so that it becomes

$$\frac{\langle P(R)\rangle}{T_{ee}}=\left[\frac{1}{T_{1e}}+\frac{1}{T_{ee}}+\frac{\omega_1^2\tau_2}{1+(\tau_2)^2(\omega_0-\delta\omega_0-\omega)^2}\right]\langle P(e)\rangle. \quad (69)$$

The equilibrium electron and rubidium polarizations are given by the simultaneous solution of Eqs. (68) and (69). It is useful to linearize Eq. (68) by expanding $A_\alpha(S)$ about the equilibrium polarizations in the absence of the radio-frequency field. Let $\langle P(R)\rangle_0$ and $\langle P(e)\rangle_0$ denote the equilibrium solutions in the absence of the radio-frequency field. Then, if we introduce the deviations from equilibrium

$$\langle\delta P(R)\rangle=\langle P(R)\rangle-\langle P(R)\rangle_0, \quad (70)$$

$$\langle\delta P(e)\rangle=\langle P(e)\rangle-\langle P(e)\rangle_0, \quad (71)$$

we can write

$$(d/dt)\langle\delta P(R)\rangle=-\left(\frac{1}{\tau}+\frac{1}{T_{1R}}+\frac{1}{T_{eR}}\right)\langle\delta P(R)\rangle+\frac{1}{T_{eR}}\langle\delta P(e)\rangle, \quad (72)$$

where we have introduced the abbreviation

$$\frac{1}{\tau}=\sigma_0\frac{\partial A_\alpha}{\partial s}\int_0^\infty I(\nu,0)d\nu. \quad (73)$$

The quantity τ is sometimes referred to as the pumping time. It is the simple relaxation time which describes the behavior of the rubidium polarization under the influence of the pumping light.

The total light transmitted by the bulb is

$$I_T=A\left(\int_0^\infty I(\nu,0)d\nu\right)(1-A_\alpha(s)), \quad (74)$$

where A is the cross-sectional area of the cylindrical absorption flask. The change in transmitted light due to a change in rubidium polarization can be written in the form

$$\delta I_T=(AN_Rz_0/\tau)\langle\delta P(R)\rangle. \quad (75)$$

Combining (68) and (69) we obtain the following equation for the rubidium polarization in the presence of the radio-frequency field:

$$\left[\frac{1}{T_{1R}}+\frac{1}{T_{eR}}-\frac{1}{T_{eR}}\left(\frac{T_{ee}^{-1}}{T_{ee}^{-1}+T_{1e}^{-1}+\omega_1^2\tau_2/[1+(\tau_2)^2(\omega_0-\delta\omega_0-\omega)^2]}\right)\right]\langle P(R)\rangle=\frac{A_\alpha(s)}{N_R z_0}\int_0^\infty I(\nu,0)d\nu. \quad (76)$$

Expanding this equation about the no radio-frequency field situation, we obtain for the change in rubidium polarization due to the radio-frequency field the equation

$$\langle\delta P(R)\rangle=-\frac{A_\alpha(s)}{N_R z_0}\left(\int_0^\infty I(\nu,0)d\nu\right)\left(\frac{1}{\tau^{-1}+T_{eR}^{-1}+T_{1R}^{-1}}\right)\left(\frac{T_{eR}^{-1}}{T_{1R}^{-1}+T_{eR}^{-1}[T_{ee}/(T_{ee}+T_{1R})]}\right)$$
$$\times\left(\frac{T_{ee}^{-1}}{T_{ee}^{-1}+T_{1e}^{-1}}\right)\left[\frac{\omega_1^2\tau_1\tau_2}{1+\omega_1^2\tau_1\tau_2+(\tau_2)^2(\omega_0-\delta\omega_0-\omega)^2}\right], \quad (77)$$

where

$$\tau_1=\frac{T_{eR}^{-1}+\tau^{-1}+T_{1R}^{-1}}{(\tau^{-1}+T_{1R}^{-1})(T_{ee}^{-1}+T_{1e}^{-1})+(T_{eR}^{-1})(T_{1e}^{-1})}. \quad (78)$$

Thus, the change in transmitted light is

$$\delta I_T=-AA_\alpha(s)\left(\int_0^\infty I(\nu,0)d\nu\right)\left(\frac{\tau^{-1}}{\tau^{-1}+T_{eR}^{-1}+T_{1R}^{-1}}\right)\left(\frac{T_{eR}^{-1}}{T_{1R}^{-1}+T_{eR}^{-1}[T_{ee}/(T_{ee}+T_{1R})]}\right)$$
$$\times\left(\frac{T_{ee}^{-1}}{T_{ee}^{-1}+T_{1e}^{-1}}\right)\left(\frac{\omega_1^2\tau_1\tau_2}{1+\omega_1^2\tau_1\tau_2+(\tau_2)^2(\omega_0-\delta\omega_0-\omega)^2}\right). \quad (79)$$

This equation indicates that the electron line will have a Lorentzian shape and a line center which is shifted by the amount $\delta\omega_0$ due to spin-exchange collisions. The direction of this shift depends upon the phase shifts and the rubidium polarization.

For the case where the electron-rubidium scattering is purely s wave and spin exchange is the only mechanism for the electron relaxation, the full width at half-maximum of the electron line will be

$$\Delta\nu=(\pi T_{ee})^{-1}=(\hbar^2/m^2v)N_R\sin^2(\delta_0^3-\delta_0^1), \quad (80)$$

and the ratio of twice the line shift to the linewidth is

$$2\delta\nu_0/\Delta\nu=P(R)\cot(\delta_0^3-\delta_0^1). \quad (81)$$

These two equations show that the linewidth and line shift are the same function of the phase shifts, that the line shift can be larger than the linewidth and that the linewidth depends only on the spin-flip cross section.

If we assume that the electron velocity distribution is a Boltzmann distribution characterized by the temperature T and that the phase shifts do not depend upon the velocity, upon averaging $\Delta\nu$ over the Boltzmann distribution we obtain the equation

$$\langle\Delta\nu\rangle_{\rm av}=N_R(\hbar/m)^2(2m/\pi kT)^{1/2}\sin^2(\delta_0^3-\delta_0^1). \quad (82)$$

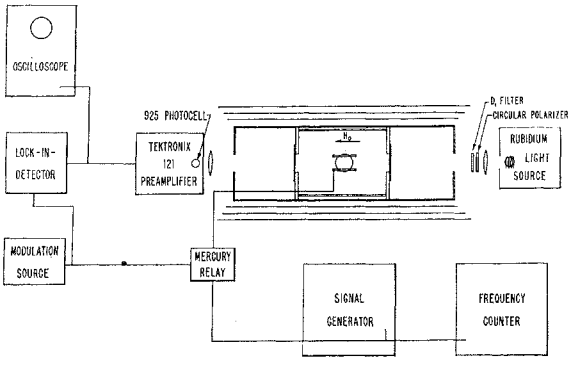

FIG. 2. Block diagram of the optical pumping apparatus.

EXPERIMENTAL TESTS OF THE THEORY

In this section of the paper we shall describe some experiments which were performed to check the spin-exchange collision theory. For this purpose, measurements were made on a simple system consisting of quasifree electrons interacting with optically pumped rubidium atoms. The large rubidium-electron spin-exchange cross section and the high velocity of room-temperature electrons make spin-exchange collisions dominate the electron relaxation. The first part of this section describes the apparatus and the second part describes the details of the measurements.

A. Apparatus

A block diagram of the optical pumping apparatus is shown in Fig. 2. The principal difference between this arrangement and that employed for other optical pumping experiments performed in this laboratory[2–4,7,8]

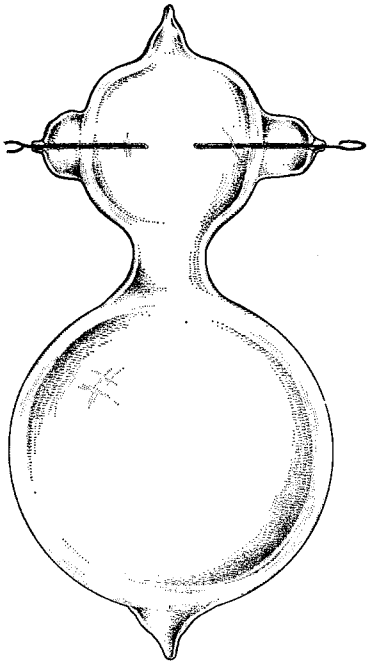

FIG. 3. A drawing of one of the absorption flasks in which the electrons were required to diffuse from the discharge region into the absorption region.

was the manner of producing the static magnetic field and of shielding the absorption flask from the perturbing influences of external magnetic fields. The field was produced by a solenoid which was 36 in. long and 13 in. in diameter. The solenoid winding consisted of two layers of No. 18 Formvar insulated copper wire. The wire was wound at the rate of 20 turns per inch into a groove which had been previously machined into an epoxy layer painted on the surface of the aluminum coil form or on the previous winding. The solenoid was placed inside three concentric magnetic shields. The shield immediately around the solenoid was $14\frac{1}{2}$ in. in diameter, 38 in. long, and made of $\frac{1}{16}$-in.-thick annealed soft iron. The next shield was $16\frac{1}{2}$ in. in diameter, 40 in. long, and made of 0.030-in.-thick mu-metal. The outermost shield was $18\frac{1}{2}$ in. in diameter, 42 in. long, and made of 0.030-in.-thick mu-metal. The ends of the solenoid were covered with $\frac{1}{4}$-in. soft iron plates. To allow passage of the light beam a 3-in.-diam hole was cut into the center of each of these iron plates. Each of the shields was provided with a set of demagnetization windings. The shields were demagnetized by passing a large ($\sim$30 A) sixty cycle current through these windings. For the experiments reported in this paper the solenoid current was derived from a mercury cell which had been packed in Styrofoam to increase its thermal stability. The magnetic field used throughout most of the experiment was 25 mG. With a good demagnetization the full width at half-maximum of the Rb^{87} Zeeman lines (700 cps/mG) in a 500-cm^3 spherical absorption flask was 40 cps.

Two types of absorption bulbs were used in this experiment. The first type were 500-cm^3 spherical absorption flasks containing rubidium atoms, a neon or argon buffer gas, and 2 Ci of tritium. The neon pressure in the neon-tritium bulb was 38.2 mm Hg; the argon pressure in the argon-tritium bulb was 36.9 mm Hg. The ionization produced by the tritium beta rays furnished a source of quasifree electrons. Calculations indicated that the electrons would rapidly thermalize so that the tritium was a source of thermal electrons. In order to check that the measurements were being made with thermal electrons, a second type of absorption flask in which the electrons were produced in a discharge and allowed to diffuse into the main part of absorption flask was constructed. Figure 3 depicts this type of flask. It consisted of a 25-cm^3 bulb mounted on the top of a 300-cm^3 bulb. The small bulb was provided with two glass-covered electrodes and free electrons were produced by a continuous radio-frequency discharge between the two electrodes. The electrons then diffused down to the main bulb. This second type of bulb was constructed with helium and neon buffer gases. The pressure in the neon bulb was 41.4 mm Hg; the pressure in the helium bulb was 40.2 mm Hg. The signals were best in the neon-tritium bulb so it was used in most of the measurements. Tests indicated that all of the bulbs gave similar results for the linewidths and frequency shifts.

The temperatures of the absorption flasks were measured with a copper-constantan thermocouple, which was attached to the side of the absorption flask. The thermocouple calibration was checked with a mercury thermometer. Solid carbon dioxide was employed to reach temperatures below room temperature. The resonance signal was measured by amplitude modulating the radio-frequency field with a mercury relay and then observing the demodulated absorption signal on a lock-in detector. The circular polarizer was arranged so that it could be quickly changed to give either right or left circularly polarized light. The vector giving the direction of the static magnetic field was parallel to the direction of motion of the photons in the light beam.

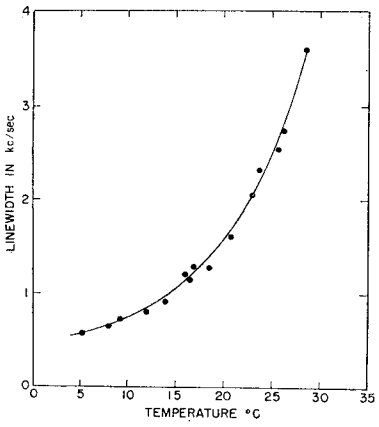

FIG. 4. Full width at half-maximum of the electron-resonance line as a function of the temperature of the absorption flask.

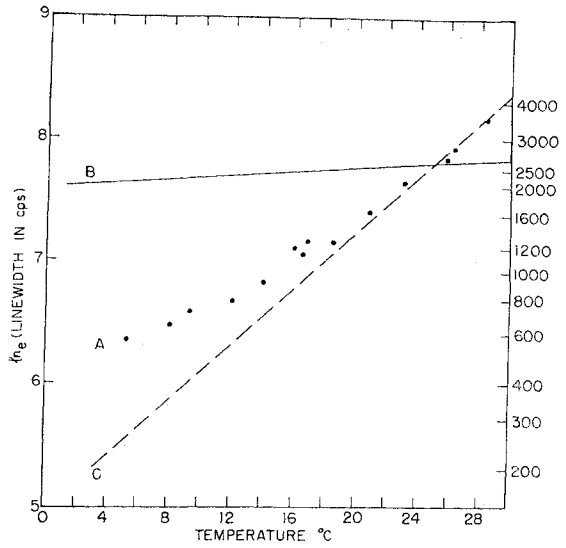

FIG. 5. A comparison of the observed temperature dependence (curve A) of the width of the electron resonance line and the temperature dependence expected from two proposed sources of the linewidth. Curve C is for a temperature dependence of the form $T^{-3/2}p(\mathrm{Rb})$, where $p(\mathrm{Rb})$ is the vapor pressure of rubidium. Curve B is for a temperature dependence of the form $T^{5/2}$. Curve C gives the expected temperature dependence if spin-exchange collisions are the dominant source of line broadening; curve B gives the expected temperature dependence if collisions with the buffer gas are the dominant source of line broadening.

B. Measurements

The first measurements were designed to determine whether of not spin-exchange collisions dominate the electron relaxation. The full width at half-maximum of the electron signal was measured as a function of temperature. In order to minimize rf broadening these measurements were made with as low a radio-frequency field as possible. The results are shown in Fig. 4. Dehmelt, in his work with electrons oriented by spin-exchange collisions with sodium atoms, concluded that collisions with the argon buffer gas were the principal source of linewidth. The sharp temperature dependence of the linewidth which we observed indicated that for an electron-rubidium system the electron linewidth was largely determined by the rubidium vapor pressure. If collisions with the buffer gas are the main relaxation mechanism,[1] one expects the linewidth to vary as $(T)^{5/2}$, where T is the absolute temperature of the electrons in the bulb. If spin-exchange collisions are more important, one expects

$$\Delta\nu \propto N(\mathrm{Rb})v_{e\mathrm{Rb}}\sigma_{\mathrm{SF}}, \tag{83}$$

where $\Delta\nu$ is the linewidth, and the other symbols have been defined previously. Inserting the temperature dependence of the various quantities, one obtains

$$\Delta\nu \propto \frac{p(\mathrm{Rb})}{T}T^{1/2}\left(\frac{1}{T}\right)=p(\mathrm{Rb})T^{-3/2}, \tag{84}$$

where $p(\mathrm{Rb})$ is the vapor pressure of the rubidium.

Figure 5 compares these two theoretical temperature dependences with the observed temperature dependence of the linewidth. The two theoretical curves were normalized to fit the data at the upper end of the temperature scale. Figure 5 indicates that the spin-exchange theory gives the better fit to the observed temperature dependence. At the lowest temperatures the experimental width is greater than one expects from spin-exchange effects. At these temperatures, temperature-independent contributions to the linewidth (e.g., an inhomogeneous magnetic field) become important. The electron linewidth due to magnetic-field inhomogeneity was approximately 100 cps. Figure 6 shows the data after the temperature independent width has been empirically subtracted out. This was accomplished by subtracting from each of the measured linewidths that width required to make the measured width at the lowest temperatures coincide with the theoretical curve. On the basis of these linewidth measurements, we conclude that the electron relaxation is dominated by spin-exchange collisions and

$$1/\tau_2=T_{ee}^{-1}+300\pi.$$

In order to further investigate the electron relaxation times, studies were made of the saturation behavior of the electron signal. Equation (79) indicates that the electron signal can be expressed in the form

$$\text{Signal amp} = (\text{const})\left\{\frac{\omega_1^2\tau_2\tau_1}{1+\omega_1^2\tau_1\tau_2+(\omega_0-\delta\omega_0-\omega)^2(\tau_2)^2}\right\}. \tag{85}$$

This equation gives methods for determining τ_2 and τ_1. In order to determine these two relaxation times,

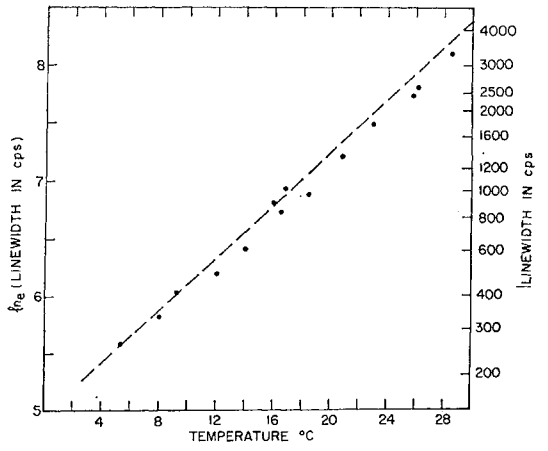

FIG. 6. A comparison of the observed linewidth with the temperature dependence expected if spin-exchange collisions are the only source of line broadening. The theoretical curve (dotted line) is the same as curve C in Fig. 5. The experimental points plotted here were derived from those plotted in Fig. 5 by subtracting the constant linewidth (~300 cycles) necessary to make the points observed at the lowest temperature fall on the theoretical curve.

measurements were made of the electron linewidth as a function of the strength of the radio-frequency field. Runs were made at various temperatures using both the tritium and the discharge bulbs. The radio-frequency field strength, ω_1, was obtained by keeping the radio-frequency oscillator set at the electron frequency, increasing the static magnetic field until the Rb^{87} signal was visible on the oscilloscope, and then photographing the rubidium signal. The rubidium signal showed the characteristic modulation of the light due to the nutation of the rubidium moment and the angular frequency ω_1 for the electron was obtained from the observed nutation frequency by using the relationship

$$\omega_1=8\pi\nu(\mathrm{Rb}^{87}). \tag{86}$$

Figure 7 shows plots of linewidth versus radio-frequency field strength for various temperatures and for the tritium bulb with a neon buffer gas. The zero radio-frequency field intercepts of the lines in Fig. 7 give the values of τ_2 for the various temperatures. The slopes of the lines give values for τ_1/τ_2. Table I summarizes the values of τ_2 obtained in the various measurements. All of the bulbs gave a value for τ_1/τ_2 in the range

$$\tau_1/\tau_2=1.0\pm0.1. \tag{87}$$

In general [Eq. (78)]

$$\tau_1=\frac{T_{eR}^{-1}+\tau^{-1}+T_{1R}^{-1}}{(\tau^{-1}+T_{1R}^{-1})(T_{ee}^{-1}+T_{1e}^{-1})+T_{eR}^{-1}T_{1e}^{-1}}.$$

Since the rubidium resonance is broadened by the light source while it is not broadened when the discharge is turned on, we conclude that

$$T_{eR}^{-1}\ll\tau^{-1}+T_{1R}^{-1}; \tag{88}$$

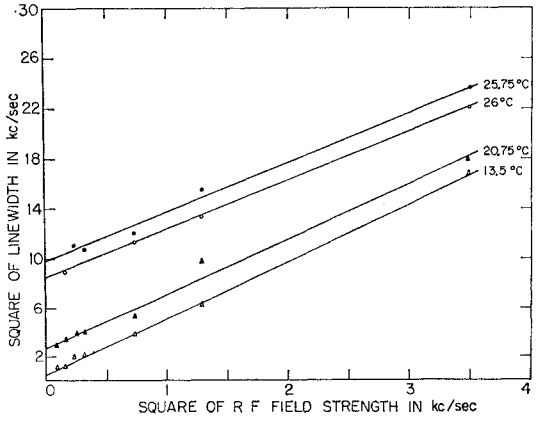

FIG. 7. Plots of the square of the electron linewidth versus the square of the radio-frequency field strength. The zero radio-frequency field intercept gives a value for τ_2 and the slope a value for τ_1/τ_2. The numbers beside the curves give the temperature of the bulb when the measurements were made. The curves at 26°C and 25.75°C indicate the reproducibility of the measurements for different runs.

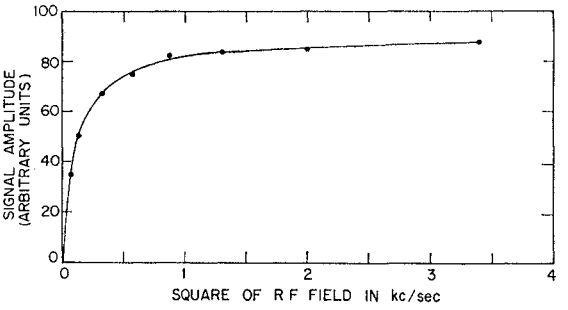

FIG. 8. A plot of the signal amplitude as a function of the square of the radio-frequency field strength. The curve shown is a fitted curve of the form $B\nu_1^2/(A+\nu_1^2)$, where ν_1 is the nutation frequency which measures the radio-frequency field strength. Values of τ_2 obtained from this type of saturation curve agreed with those obtained from the curves shown in Fig. 7.

Then also noting that spin-exchange collisions constitute the main source of the electron linewidth, we obtain

$$\tau_1\simeq\frac{\tau^{-1}+T_{1R}^{-1}}{(\tau^{-1}+T_{1R}^{-1})(T_{ee}^{-1}+T_{1e}^{-1})}=\frac{1}{T_{ee}^{-1}+T_{1e}^{-1}}. \tag{89}$$

From this equation and the experimental value for τ_1/τ_2 we obtain the equation

$$\tau_2^{-1}\simeq T_{ee}^{-1}+T_{1e}^{-1}, \tag{90}$$

and from the dependence of the τ_2 on the temperature we obtain the relation

$$T_{1e}\simeq 1/300\pi.$$

TABLE I. The values of τ_2 obtained for various bulbs and various bulb temperatures. The values of τ_2 referred to 20°C were obtained from the equation

$$\tau_2(20°\mathrm{C})=\frac{N(\mathrm{Rb\ at}\ T)}{N(\mathrm{Rb\ at}\ 20°\mathrm{C})}\tau_2(T).$$

Here $N(\mathrm{Rb\ at}\ T)$ is the number of rubidium atoms/cm³ at temperature T.

Bulb type	Temperature in °C	τ_2 in sec	τ_2 referred to 20°C
Neon-Tritium	12	4.9×10^{-4}	1.9×10^{-4}
Neon-Tritium	13.5	4.5×10^{-4}	2.2×10^{-4}
Neon-Tritium	14	3.8×10^{-4}	1.9×10^{-4}
Neon-Tritium	20	1.9×10^{-4}	1.9×10^{-4}
Neon discharge	20	2.4×10^{-4}	2.4×10^{-4}
Neon-Tritium	26	1.0×10^{-4}	1.85×10^{-4}

This gives the order of magnitude of the electron relaxation which is not strongly dependent upon temperature. If it is assumed that 100 cps of the 300-cps temperature-independent portion of the linewidth is due to magnetic-field inhomogeneity, this leaves 200 cps of the residual linewidth unexplained. This could be due to interaction with the buffer gas. In his experiment on electron-sodium spin-exchange collisions in an argon buffer gas (70 mm Hg argon), Dehmelt attributed 5 kc/sec of the linewidth to electron-argon collisions.

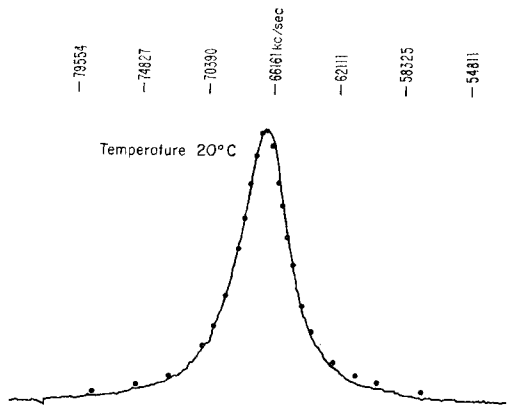

FIG. 9. A recorder tracing of one of the electron lines. For this recording the modulation frequency was 10 cps, the lock-in-detector time constant was 0.03 sec, and the temperature of the bulb was 20°C. The full width at half-maximum of this curve is 3760 cps. The width due to magnetic field inhomogeneity was approximated 100 cps the width due to spin-exchange collisions 1500 cps. The dots indicate a Lorentzian fit to the experimental curve.

TABLE II. Measured values of the frequency shift. The tritium in neon bulb (38.2 mm Hg neon) was used for these measurements. For these measurements the rubidium polarization was always greater than 90%.

Bulb temperature in °C	$\delta\nu_0$ Shift in cps	$\Delta\nu$ Linewidth in cps	$\frac{\delta\nu_0}{\Delta\nu}$	$\frac{\delta\nu_0}{\Delta\nu-300}$
10	−10	730	−0.014	−0.023
16	−20	1100	−0.018	−0.025
16.7	−28	1200	−0.023	−0.031
17.5	−20	1250	−0.016	−0.021
17.8	−32	1270	−0.025	−0.033
18.5	−23	1350	−0.017	−0.022
18.9	−33	1400	−0.024	−0.030
19.3	−30	1450	−0.021	−0.026
20	−35	1500	−0.021	−0.029
20.7	−37	1620	−0.023	−0.028
21.1	−30	1650	−0.018	−0.022
21.3	−30	1670	−0.018	−0.022
21.8	−47	1800	−0.026	−0.031
22.4	−31	1950	−0.016	−0.019
22.6	−36	2000	−0.015	−0.021
22.9	−36	2050	−0.018	−0.021
27	−60	3000	−0.022	−0.022

Our measurements indicate a much smaller interaction with the buffer gas.

Measurements were also made of the signal amplitude for various strengths of the radio-frequency field. Figure 8 shows a typical plot of signal amplitude versus the strength of the radio-frequency field. A second value for τ_2 was determined from these measurements. The values of τ_2 obtained in this fashion agreed with those obtained from the linewidth measurements.

In order to study the line shape of the electron resonance a lock-in detector was used to record the shape of the line. A typical recorder tracing is shown in Fig. 9. Figure 9 also shows a Lorentzian fit to the observed line shape. It is apparent that the line is well represented by the Lorentzian shape.

The other major aspect of the theoretical expression to be verified is the predicted frequency shift. The frequency shift was measured by first observing the electron resonance frequency with left circularly polarized light and then with right circularly polarized light. This operation changes the sign of the rubidium polarization and consequently the direction of the shift. The shift was then determined from the equation

$$\delta\nu_0 = \frac{\nu(\text{left}) - \nu(\text{right})}{2}. \tag{91}$$

This sequence of measurements was repeated until a precise value for the shift was obtained. Measurements of the Rb^{87} Zeeman frequency were interspersed to correct for any drifts in the magnetic field. The electron resonance frequency was smaller when left circularly polarized light was incident on the bulb. For this situation the rubidium polarization was positive. For bulb temperatures less than 35°C, the rubidium polarization was greater than 90%. The measured values of the shift are summarized in Table II. No shifts greater than 3 cps were observed in the rubidium resonance frequency when the circular polarizer was switched from right to left circular polarization. Figure 10 shows a plot of the absolute value of the shift in the electron frequency versus temperature. For comparison there is also shown the variation with temperature of the rubidium density in the bulb. Figure 10 indicates that the shift depends upon the rubidium density. Table II shows that the shift divided by the linewidth varies slowly with temperature.

From the experimental measurements we conclude that the form of the theoretical expression for the optical pumping signal is correct. It remains only to determine the magnitude of the spin-flip cross section,

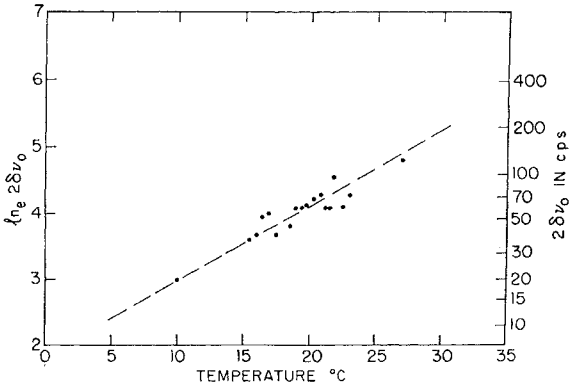

FIG. 10. A plot of twice the absolute value of the shift versus the temperature of the absorption flask. The dashed curve gives the expected temperature dependence if the shift is due to spin-exchange collisions. For the bulb temperatures used in these measurements the rubidium polarization was always greater than 90%. The electron resonance frequency was greater when right circularly polarized light was incident on the absorption flask.

and to see if the magnitude of the shift is physically reasonable. The spin-flip cross section can be determined either from the measured value of T_{ee} or from the ratio of the frequency shift to the linewidth. The first method requires knowledge of the rubidium density in the bulb; the second method does not depend upon the rubidium density, as long as the rubidium polarization is constant. There are at present in the literature several expressions for the vapor pressure of rubidium. The rubidium density versus temperature derived from three[22–24] of these expressions is shown in Fig. 11.

Rather than calculate the cross section, we shall use the formula

$$\langle\Delta\nu\rangle_{\rm av}=N_{\rm Rb}\left(\frac{\hbar}{mc}\right)^2 c\left(\frac{2mc^2}{\pi kT}\right)^{1/2} S(\delta^3-\delta^1)\,, \qquad (92)$$

where

$$S(\delta^3-\delta^1)=\sum_{l=0}^{\infty}(2l+1)\sin^2(\delta_l{}^3-\delta_l{}^1)\,, \qquad (93)$$

to calculate the phase shift sum, $S(\delta^3-\delta^1)$. Equation (92) is the linewidth averaged over a Boltzmann distribution for the electrons assuming that the phase shifts do not vary with the electron velocity. If we use the data in Table I and subtract out the 300-cps linewidth which seems to arise from sources other than spin-exchange collisions, we conclude that for $T=20$°C

$$\langle\Delta\nu\rangle_{\rm av}=1300\pm100 \text{ cps}.$$

If we insert this expression into Eq. (92) and use the value of the rubidium density from curve A in Fig. 11, we obtain

$$\sum_{l=0}^{\infty}(2l+1)\sin^2(\delta_l{}^3-\delta_l{}^1)=1.1\pm0.1\,. \qquad (94)$$

Figure 12 shows the value of this phase-shift sum for various values of the s- and p-wave phase shifts.

If we assume that both s- and p-wave phase shifts are present then the theoretical expression for the ratio of twice the shift to the linewidth [Eq. (26)] is

$$\kappa=\frac{1\sin2(\delta_0{}^3-\delta_0{}^1)+3\sin2(\delta_1{}^3-\delta_1{}^1)}{2\sin^2(\delta_0{}^3-\delta_0{}^1)+3\sin^2(\delta_1{}^3-\delta_1{}^1)}\,. \qquad (95)$$

This equation shows that κ is a function only of $(\delta_0{}^3-\delta_0{}^1)$ and $(\delta_1{}^3-\delta_1{}^1)$. Figure 13 gives the behavior of κ as a function of these two parameters. From Table II we conclude that experimentally

$$\kappa=+0.05\pm0.01\,.$$

From the measured value of $S(\delta^3-\delta^1)$ and the measured value of κ we conclude that

$$\delta_0{}^3-\delta_0{}^1=-\tfrac{1}{2}\pi-\epsilon\,; \qquad (96)$$

or

$$\delta_0{}^3-\delta_0{}^1=\tfrac{1}{2}\pi-\epsilon\,, \qquad (97)$$

where ϵ is positive and small. In addition $(\delta_1{}^3-\delta_1{}^1)$ is small. This solution is quite reasonable physically. One expects the attraction between the rubidium and the electron to be greater in the singlet than in the triplet state. A mass spectrometer measurement in which the Rb^- ion was observed has been reported.[25] If the singlet state of the Rb^- ion is bound and the triplet state is unbound, the proper zero-energy phase shifts

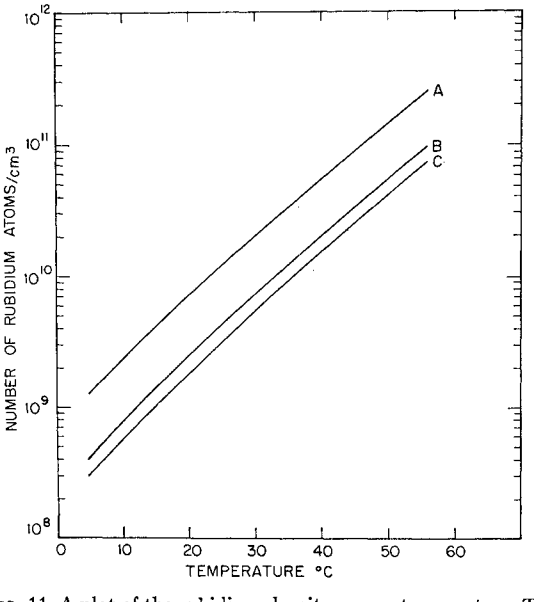

FIG. 11. A plot of the rubidium density versus temperature. The expressions used were:

Curve A[24] $\log_{10}p(\text{Rb})=-4302/T+11.722-1.5\log_{10}T$;
Curve B[23] $\log_{10}p(\text{Rb})=-4560/T+12.00-1.45\log_{10}T$;
Curve C[22] $\log_{10}p(\text{Rb})=-4558/T+11.985-1.45\log_{10}T$.

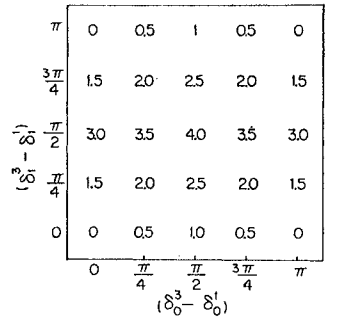

FIG. 12. A plot of the expression $[\sin^2(\delta_0{}^3-\delta_0{}^1)+3\sin^2(\delta_1{}^3-\delta_1{}^1)]$ versus the s-and p-wave singlet and triplet phase shifts. The spin-flip cross section is given by multiplying this expression by π/k^2.

[22] G. G. Grau and K. L. Schaefer, *Landolt-Börnstein Zahlenwerte und Funktionen Aus Physik, Chemie, Astronomie, Geophysik, und Technik* (Springer-Verlag, Berlin, 1960), Vol. II, p. 7.

[23] *Metals Reference Handbook*, edited by Colin J. Smithells (Butterworths Scientific Publications Ltd., London, 1955), Vol. II, p. 613.

[24] R. W. Ditchburn and J. C. Gilmour, Rev. Mod. Phys. **13**, 310 (1941).

[25] V. M. Dukel'skil, E. Yo Zondberg, and N. J. Ionov, Dokl. Akad. Nauk S.S.S.R. **62**, 232 (1948). (This paper can be obtained in translation from the Chief, Photoduplication Service, Library of Congress, Washington, D. C., using the reference number RT 2125.)

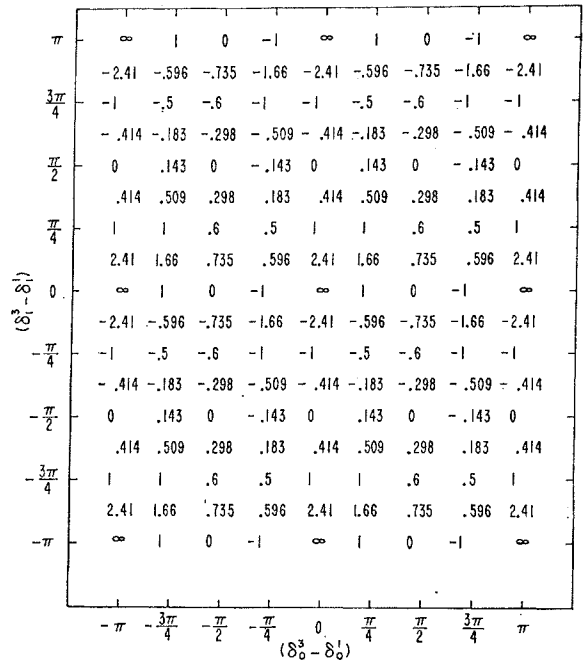

FIG. 13. A plot of the shift parameter κ versus the s- and p-wave singlet and triplet phase shifts. In terms of these phase shifts

$$\kappa=\frac{2\,\delta\nu_0}{(\Delta\nu)P(R)}=\frac{1}{2}\frac{\sin 2(\delta_0^3-\delta_0^1)+3\sin 2(\delta_1^3-\delta_1^1)}{\sin^2(\delta_0^3-\delta_0^1)+3\sin^2(\delta_1^3-\delta_1^1)}.$$

are 5π for both singlet and triplet s-wave scattering. Both phase shifts ultimately decrease as the energy increases. If there is a singlet bound state near zero energy, the singlet phase shift becomes $\frac{9}{2}\pi$ and the triplet $5\pi-\epsilon$, Hence,

$$\delta_0^3-\delta_0^1=5\pi-\epsilon-\tfrac{9}{2}\pi=\tfrac{1}{2}\pi-\epsilon.$$

On this basis $(\delta_0^3-\delta_0^1)$ would be given by Eq. (97). A measurement of the total cross section for thermal electrons colliding with rubidium such as has been reported for electrons on cesium[26] would give a check on this hypothesis and permit a determination of both singlet and triplet phase shifts. It is interesting to note that in his work on electron-sodium collisions,[1] Dehmelt also concluded that $\delta_0^1\simeq\frac{1}{2}\pi$, that singlet-$s$ scattering was dominant, and that the cross section was near the theoretical maximum.

CONCLUSION

A theory has been devised to account for the nuclear and electron relaxation due to spin-exchange collisions. This theory predicts a frequency shift in addition to a linewidth. The frequency shift and linewidth both depend upon the same combinations of the singlet and triplet phase shifts. The existence of the frequency shift makes it possible to measure spin-exchange cross sections when the density of atoms is not known. Rather than determining the cross section from the density and linewidth, one can determine it from the ratio of the frequency shift to the linewidth. This removes one of the most difficult aspects of measuring spin-exchange cross sections.

When Lewis[14] derived his expression for the frequency shift, he replaced the rubidium-electron interaction with a delta-function interaction of the proper strength and calculated the expectation value for the energy of the electron in a gas of rubidium atoms. He assumed that the part of the energy which depended upon the rubidium polarization and the collision cross section gave the proper value for the energy shift. This method essentially replaces a time average by an average over phase space. In a spin-exchange collision there is a high probability of a spin-flip and consequently the time average cannot be simply replaced by a phase-space average.

ACKNOWLEDGMENTS

We are particularly indebted to Professor Kurt Gottfried and to David Ross for numerous conversations concerning the proper way to treat the change in the density matrix, and the general theory of pressure broadening. We wish to thank Dr. James Hobart for sending us a copy of his thesis.

APPENDIX A

Application to the Actual Rubidium Isotopes

In this appendix we will consider the case of one of the actual rubidium isotopes colliding with quasifree electrons. For this purpose we will choose Rb^{87} which has a nuclear spin of $\frac{3}{2}$. The results of our analysis can easily be extended to Rb^{85} which has spin $\frac{5}{2}$. The exact behavior of the rubidium density matrix will depend upon the spectrum of the light source, the filtering of light by the bulb, the rubidium-rubidium spin-exchange collisions, the amount of reorientation in the optically excited state; the spin-exchange collisions with the electrons, and the relaxation processes which restore the rubidium populations to equilibrium. To analyze all of these in complete detail is a difficult problem for whose solution there is not sufficient data at the present time. In our analysis we shall show that when the absorption flask is illuminated with $D_1(5P_{1/2}\rightarrow 5S_{1/2})$ resonance radiation, the total light absorption and the driving force for the spin-exchange orientation of the electrons are the same function of the diagonal elements of the rubidium density matrix. On this basis we expect that the optical signals for electrons in spin-exchange equilibrium with the real rubidium isotopes will be very similar to those for the spin-zero rubidium model.

We will first consider the optical absorption. If we have an optical transition between an atomic ground state characterized by the quantum numbers F_g, M_g, I, J_g, L_g, S and an excited state characterized by the

[26] C. L. Chen and M. Raether, Phys. Rev. **128**, 2679 (1962).

quantum numbers F_e, M_e, I, J_e, L_e, S, the total cross section for the absorption of circularly polarized light is

$$\int_0^\infty \sigma_\kappa(F_g, M_g, I, J_g, L_g, S \rightarrow F_e, M_e, I, J_e, L_e, S)d\nu = \frac{3}{8\pi}\frac{\lambda^2}{\tau}\frac{(2F'_g+1)|W(J_gJ_eF_gF_e;1I)|^2}{\sum_{F_g}(2F'_g+1)|W(J_gJ_eF_gF_e;1I)|^2} \times|C(F_g1F_e;M_g\kappa M_e)|^2 \quad \text{(A1)}$$

where $W(J_gJ_eF_gF_e;1I)$ is a Racah coefficient, $C(F'_g1F'_e;M_g\kappa M_e)$ is a Clebsch-Gordan coefficient,[27] λ is the wavelength of the radiation, τ is the lifetime of the excited state and κ is $+1$ for left circularly polarized light and -1 for right circularly polarized light. This expression can be conveniently rewritten in terms of the intensities of the hyperfine lines in the multiplet. In this form it is

$$\int_0^\infty \sigma_\kappa(F_g, J_g, M_g \rightarrow F_e, J_e, M_e)d\nu = \frac{3}{8\pi}\frac{\lambda^2}{\tau}|C(F_g1F_e;M_g\kappa M_e)|^2 \times\frac{\text{Intensity of } (F_e'J_e\rightarrow F_gJ_g) \text{ emission line}}{\text{Total intensity of all emission lines from } F_e'J_e \text{ level}}. \quad \text{(A2)}$$

Using this expression the standard tables of multiplet intensities can be used to calculate the absorption cross sections. The actual cross section will have a Doppler shape of the form

$$\sigma_\kappa(\nu)=\sigma_{0\kappa}(F_g,J_g,M_g;F_e,J_e,M_e)\times e^{-4\ln2[\nu-\nu(F_gJ_g\rightarrow F_eJ_e)/\Delta\nu_D]^2}, \quad \text{(A3)}$$

where

$$\sigma_{0\kappa}(F_g, J_g, M_g \rightarrow F_e, J_e, M_e) = \frac{2(\ln2)^{1/2}}{\pi^{1/2}\Delta\nu_D}\int_0^\infty \sigma_\kappa(F_g, J_g, M_g \rightarrow F_e, J_e, M_e)d\nu. \quad \text{(A4)}$$

TABLE III. The optical absorption cross sections of the various magnetic substates of Rb^{87} for left circularly polarized $D_1(5P_{1/2}\rightarrow 5S_{1/2})$ optical resonance radiation. The numbers in the table are relative cross sections and should be multiplied by

$$\frac{1}{16\pi}\frac{\lambda^2}{\tau}\frac{2(\ln2)^{1/2}}{\pi^{1/2}\Delta\nu_D}\exp\left[-4\ln2\left(\frac{\nu-\nu_0}{\Delta\nu_D}\right)^2\right]$$

to obtain the magnitude of the cross section.

State	2, 2	2, 1	2, 0	2, −1	2, −2	1, −1	1, 0	1, 1
Relative cross section	0	1	2	3	4	1	2	3

[27] M. E. Rose, *Elementary Theory of Angular Momentum* (John Wiley & Sons, Inc., New York, 1957), pp. 32–124.

The absorption cross sections for the various magnetic substates of Rb^{87} when it is illuminated by left circularly polarized D_1 resonance radiation are summarized in Table III. If we assume that all the optical hyperfine transitions have the same frequency we can write the light absorption for the cylindrical bulb of Fig. 1 in the form

$$\frac{\partial I(\nu,z)}{\partial z}=-\frac{N(Rb^{87})\sigma_T(\nu)}{2}[\rho_{22}(Rb^{87})+2\rho_{33}(Rb^{87})+3\rho_{44}(Rb^{87})+4\rho_{55}(Rb^{87})+\rho_{66}(Rb^{87})+2\rho_{77}(Rb^{87})+3\rho_{88}(Rb^{87})], \quad \text{(A5)}$$

where $\rho_{ii}(Rb^{87})$ are the diagonal elements of the density matrix for Rb^{87}, where the indices 1, 2, 3, 4, 5, 6, 7, 8 refer to the states (2,2), (2,1), (2,0), (2, −1), (2, −2), (1, −1), (1,0), (1,1), respectively, and where $\sigma_T(\nu)$ is given by the equation

$$\sigma_T(\nu)=\frac{1}{8\pi}\frac{\lambda^2}{\tau}\frac{2(\ln2)^{1/2}}{\pi^{1/2}(\Delta\nu_D)}e^{-4\ln2[(\nu-\nu_0)/\Delta\nu_D]^2}. \quad \text{(A6)}$$

If we introduce the electron polarization for Rb^{87} through the defining equation

$$P_e(Rb^{87})=\mathrm{Tr}[\sigma_{ez}\rho(Rb^{87})], \quad \text{(A7)}$$

where σ_{ez} is the Pauli spin matrix which operates on the electron coordinate, then we can write

$$\frac{\partial I(\nu,z)}{\partial z}=-N(Rb^{87})\sigma_T(\nu)[1-P_e(Rb^{87})]. \quad \text{(A8)}$$

This equation is very similar to Eq. (61) and can be solved and averaged in a similar way. If we introduce

$$P_e(Rb)=\frac{N(Rb^{85})}{N(Rb^{85})+N(Rb^{87})}\mathrm{Tr}[\sigma_{ez}\rho(Rb^{85})]+\frac{N(Rb^{87})}{N(Rb^{85})+N(Rb^{87})}\mathrm{Tr}[\sigma_{ez}\rho(Rb^{87})], \quad \text{(A9)}$$

we can write for the total transmitted light

$$I_T=A\left(\int_0^\infty I(\nu,0)d\nu\right)(1-A_\alpha(S)), \quad \text{(A10)}$$

where

$$S=[N(Rb^{85})+N(Rb^{87})]\sigma_T z_0[1-P_e(Rb)]. \quad \text{(A11)}$$

A comparison of Eqs. (66) and (74) with (A10) and (A11) shows the relationship between the rubidium model with no nuclear spin and the actual rubidium.

Now we wish to consider spin-exchange collisions between Rb^{87} and the quasifree electrons. If we neglect the effects of the nuclear spin in the collisions and assume that the temperature is high enough that one

TABLE IV. The matrix $\boldsymbol{\sigma}(\mathrm{Rb}^{87})\cdot\boldsymbol{\sigma}(e)$.

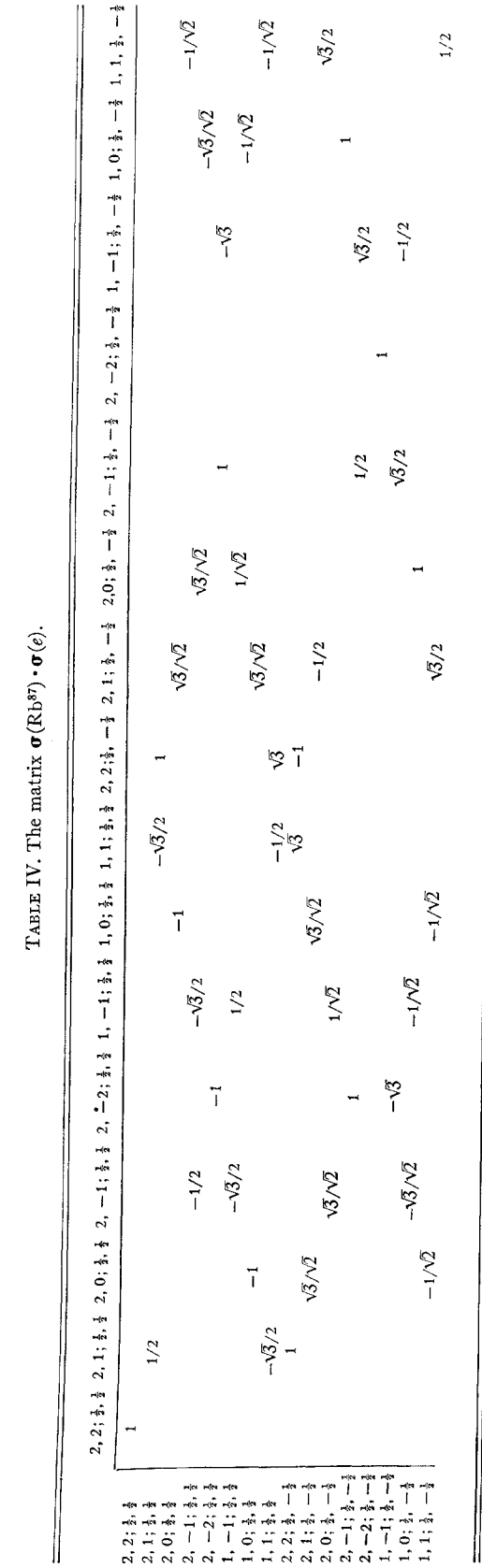

does not have to worry about the conservation of energy in the hyperfine transitions, Eq. (27) can be used to calculate the change in the electron and rubidium density matrices. We need only deal with the full 8×8 density matrix for the Rb. The matrix for $\boldsymbol{\sigma}(\mathrm{Rb}^{87})\cdot\boldsymbol{\sigma}(e)$ is listed in Table IV. A straightforward calculation using this matrix and Eq. (27) for the case where the rubidium density matrix is diagonal and the electron matrix has off-diagonal elements shows that

$$\frac{d\rho(e)}{dt}=\begin{bmatrix} \dfrac{P_e(\mathrm{Rb}^{87})-P(e)}{2T_{ee}} & -\dfrac{1-i\kappa P_e(\mathrm{Rb}^{87})}{T_{ee}}\rho_{12}(e) \\ -\dfrac{1+i\kappa P_e(\mathrm{Rb}^{87})}{T_{ee}}\rho_{21}(e) & \dfrac{P(e)-P(\mathrm{Rb}^{87})}{2T_{ee}} \end{bmatrix}, \tag{A12}$$

where

$$1/T_{ee}=v_{e\mathrm{Rb}^{87}}N(\mathrm{Rb}^{87})\sigma_{\mathrm{SF}}, \tag{A13}$$

and that for the electronic polarization of the rubidium

$$\frac{dP_e(\mathrm{Rb}^{87})}{dt}=\frac{P(e)-P_e(\mathrm{Rb}^{87})}{T_{e\mathrm{Rb}^{87}}}, \tag{A14}$$

where

$$1/T_{e\mathrm{Rb}^{78}}=v_{e\mathrm{Rb}^{87}}N(e)\sigma_{\mathrm{SF}}. \tag{A15}$$

A similar set of equations can be derived for collisions between Rb^{85} and the electrons. We conclude that for electrons colliding with rubidium atoms, the Rb^{87} and Rb^{85} can be replaced by an equivalent spin one-half system whose electronic polarization is equal to the electronic polarization of the rubidium.

APPENDIX B

Application to Other Systems

It is instructive to calculate the change in the density matrix due to spin-exchange collisions for systems more complicated than the electron spin system. The main purpose of this investigation is to determine the pattern of the frequency shifts and the spin-exchange linewidths for more complicated systems. First consider the case of collisions between polarized electrons and hydrogen atoms. We shall assume that there are no off-diagonal elements of the electron density matrix and then calculate the change in the hydrogen density matrix for the cases where we have a single radio-frequency field present. We will use e_{ij} to denote the elements of the electron density matrix, H_{ij} to denote the elements of the hydrogen density matrix, and $P(e)$ to denote the electron polarization. For the hydrogen density matrix the indices 1, 2, 3, and 4 denote the states (1,1), (1,0), (1, −1), and (0,0), respectively. The matrix for $\boldsymbol{\sigma}(\mathrm{H})\cdot\boldsymbol{\sigma}(e)$ is summarized in Table V. Using this matrix the change in the hydrogen density matrix due to spin-exchange collisions with

TABLE V. The matrix $\boldsymbol{\sigma}(\mathrm{H})\cdot\boldsymbol{\sigma}(e)$. The state labels are written so that the first two numbers give the state of the hydrogen atom and the last two the state of the electron.

	$1,1;\frac{1}{2},\frac{1}{2}$	$1,0;\frac{1}{2},\frac{1}{2}$	$1,-1;\frac{1}{2},\frac{1}{2}$	$0,0;\frac{1}{2},\frac{1}{2}$	$1,1;\frac{1}{2},-\frac{1}{2}$	$1,0;\frac{1}{2},-\frac{1}{2}$	$1,-1;\frac{1}{2},-\frac{1}{2}$	$0,0;\frac{1}{2},-\frac{1}{2}$
$1,1;\frac{1}{2},\frac{1}{2}$	1							
$1,0;\frac{1}{2},\frac{1}{2}$				1	$\sqrt{2}$			
$1,-1;\frac{1}{2},\frac{1}{2}$			-1			$\sqrt{2}$		$\sqrt{2}$
$0,0;\frac{1}{2},\frac{1}{2}$		1			$-\sqrt{2}$			
$1,1;\frac{1}{2},-\frac{1}{2}$		$\sqrt{2}$		$-\sqrt{2}$	-1			
$1,0;\frac{1}{2},-\frac{1}{2}$			$\sqrt{2}$					-1
$1,-1;\frac{1}{2},-\frac{1}{2}$							1	
$0,0;\frac{1}{2},-\frac{1}{2}$			$\sqrt{2}$			-1		

TABLE VI. The expression $\mathrm{Tr}_e[-3\rho+(1+2i\kappa)(\boldsymbol{\sigma}_e\cdot\boldsymbol{\sigma}_\mathrm{H})\rho+(1-2i\kappa)\rho(\boldsymbol{\sigma}_e\cdot\boldsymbol{\sigma}_\mathrm{H})+(\boldsymbol{\sigma}_e\cdot\boldsymbol{\sigma}_\mathrm{H})\rho(\boldsymbol{\sigma}_e\cdot\boldsymbol{\sigma}_\mathrm{H})]$ for a spin-exchange collision between polarized electrons and hydrogen atoms. When multiplied by $\frac{1}{4}v_{e\mathrm{H}}N(e)\sigma_{\mathrm{SF}}$ this matrix gives the time rate of change of the hydrogen density matrix due to spin-exchange collisions. This matrix is a summary of several calculations and is valid when one set of off-diagonal elements, such as H_{24} and H_{42}, is not equal to zero.

	1, 1	1, 0	1, −1	0, 0
1, 1	$-4e_{22}\mathrm{H}_{11}+2e_{11}\mathrm{H}_{22}$ $+2e_{11}\mathrm{H}_{44}$ $-2e_{11}(\mathrm{H}_{42}+\mathrm{H}_{24})$	$[-3+(1+i\kappa)P(e)]\mathrm{H}_{12}$		$[-3+(1+i\kappa)P(e)]\mathrm{H}_{14}$
1, 0	$[-3+(1-i\kappa)P(e)]\mathrm{H}_{21}$	$-3\mathrm{H}_{22}+\mathrm{H}_{44}$ $+2e_{22}\mathrm{H}_{11}+2e_{11}\mathrm{H}_{33}$ $+[\mathrm{H}_{24}+\mathrm{H}_{42}+i\kappa(\mathrm{H}_{42}-\mathrm{H}_{24})]P(e)$	$[-3-(1-i\kappa)P(e)]\mathrm{H}_{23}$	$-3\mathrm{H}_{24}+\mathrm{H}_{42}$ $+2e_{11}\mathrm{H}_{33}-2e_{22}\mathrm{H}_{11}$ $+[\mathrm{H}_{44}+\mathrm{H}_{22}+i\kappa(\mathrm{H}_{44}-\mathrm{H}_{22})]P(e)$
1, −1		$[-3-(1+i\kappa)P(e)]\mathrm{H}_{32}$	$-4e_{11}\mathrm{H}_{33}+2e_{22}\mathrm{H}_{22}$ $+2e_{22}\mathrm{H}_{44}$ $+2e_{22}[\mathrm{H}_{42}+\mathrm{H}_{24}]$	$[-3-(1+i\kappa)P(e)]\mathrm{H}_{34}$
0, 0	$[-3+(1-i\kappa)P(e)]\mathrm{H}_{41}$	$-3\mathrm{H}_{42}+\mathrm{H}_{24}$ $+2e_{11}\mathrm{H}_{33}-2e_{22}\mathrm{H}_{11}$ $+[\mathrm{H}_{44}+\mathrm{H}_{22}-i\kappa(\mathrm{H}_{44}-\mathrm{H}_{22})]P(e)$	$[-3-(1-i\kappa)P(e)]\mathrm{H}_{43}$	$-3\mathrm{H}_{44}+\mathrm{H}_{22}$ $+2e_{22}\mathrm{H}_{11}+2e_{11}\mathrm{H}_{33}$ $+[\mathrm{H}_{24}+\mathrm{H}_{42}+i\kappa(\mathrm{H}_{24}-\mathrm{H}_{42})]P(e)$

TABLE VII. The expression $\mathrm{Tr}_e[-3\rho+(1+2i\kappa)(\boldsymbol{\sigma}(e)\cdot\boldsymbol{\sigma}(\mathrm{H}))\rho+(1-2i\kappa)\rho(\boldsymbol{\sigma}(e)\cdot\boldsymbol{\sigma}(\mathrm{H}))+(\boldsymbol{\sigma}(e)\cdot\boldsymbol{\sigma}(\mathrm{H}))\rho(\boldsymbol{\sigma}(e)\cdot\boldsymbol{\sigma}(\mathrm{H}))]$ after the terms which will average to zero have been discarded. When multiplied by $\frac{1}{4}v_{e\mathrm{H}}N(e)\sigma_{\mathrm{SF}}$ this matrix gives the time rate of change of the hydrogen density matrix due to spin-exchange collisions with polarized electrons. This matrix is a summary of several calculations and is valid when only one set of off-diagonal elements, such as H_{24} and H_{42}, is not equal to zero.

	1, 1	1, 0	1, −1	0, 0
1, 1	$-4e_{22}\mathrm{H}_{11}$ $+2e_{11}[\mathrm{H}_{22}+\mathrm{H}_{44}]$	$[-3+(1+i\kappa)P(e)]\mathrm{H}_{12}$		$[-3+(1+i\kappa)P(e)]\mathrm{H}_{14}$
1, 0	$[-3+(1-i\kappa)P(e)]\mathrm{H}_{21}$	$-3\mathrm{H}_{22}+\mathrm{H}_{44}$ $+2[e_{22}\mathrm{H}_{11}+e_{11}\mathrm{H}_{33}]$	$[-3-(1-i\kappa)P(e)]\mathrm{H}_{23}$	$-3\mathrm{H}_{24}+\mathrm{H}_{42}$
1, −1		$[-3-(1+i\kappa)P(e)]\mathrm{H}_{32}$	$-4e_{11}\mathrm{H}_{33}$ $+2e_{22}[\mathrm{H}_{22}+\mathrm{H}_{44}]$	$[-3-(1+i\kappa)P(e)]\mathrm{H}_{34}$
0, 0	$[-3+(1-i\kappa)P(e)]\mathrm{H}_{41}$	$-3\mathrm{H}_{42}+\mathrm{H}_{24}$	$[-3-(1-i\kappa)P(e)]\mathrm{H}_{43}$	$-3\mathrm{H}_{44}+\mathrm{H}_{22}$ $+2e_{22}\mathrm{H}_{11}+2e_{11}\mathrm{H}_{33}$

polarized electrons can be calculated from Eq. (27). The result of this calculation is summarized in Table VI. As written this matrix is the summary of five independent calculations and it is only valid when one pair of off-diagonal matrix elements such as H_{21} and H_{12} is present. Also for this calculation we have assumed that the time is fixed and that we have one particular value for the off-diagonal matrix elements. In general the off-diagonal elements will vary with time and only those collision produced additional terms which have the correct time dependence will give a contribution to the change of the off-diagonal elements. If we set equal to zero those terms with the incorrect time dependence, the equations simplify. The simplified expression for the change in the hydrogen density matrix is summarized in Table VII. Table VII indicates that the frequency of the $(1,0)\rightarrow(0,0)$ transition will not be shifted, that the $(1,1)\rightarrow(0,0)$ and the $(1,-1)\rightarrow(0,0)$ transitions will be shifted in opposite directions, that the $(1,1)\rightarrow(1,0)$ and the $(1,0)\rightarrow(1,1)$ transitions

TABLE VIII. The expression $\mathrm{Tr}_e[-3\rho+(1-2i\kappa)\boldsymbol{\sigma}(\mathrm{Rb})\cdot\boldsymbol{\sigma}(e)\rho+(1-2i\kappa)\rho\boldsymbol{\sigma}(\mathrm{Rb})\cdot\boldsymbol{\sigma}(e)+(\boldsymbol{\sigma}(\mathrm{Rb})\cdot\boldsymbol{\sigma}(e))\rho\boldsymbol{\sigma}(\mathrm{Rb})\cdot\boldsymbol{\sigma}(e)]$ after the terms which will average to zero have been discarded. When multiplied by $\frac{1}{4}v_eRN(e)\sigma_{SF}$ this matrix gives the time rate of change of the rubidium density matrix due to spin-exchange collisions with polarized electrons. This matrix summarizes 15 separate calculations and is valid only when one pair of off-diagonal matrix elements (e.g., R_{34} and R_{43}) is not equal to zero.

	2, 2	2, 1	2, 0	2, −1	2, −2	1, −1	1, 0	1, 1
2, 2	$[-2+2P(e)]R_{11}$ $+e_{11}(R_{22}+3R_{88})$	$[-\frac{5}{2}+$ $(\frac{3}{2}+i\kappa)P(e)]R_{12}$						$[-\frac{7}{2}+$ $(\frac{1}{2}+3i\kappa)P(e)]R_{13}$
2, 1	$[-\frac{5}{2}+$ $(\frac{3}{2}-i\kappa)P(e)]R_{21}$	$[-(11/4)+P(e)]R_{22}$ $+\frac{3}{4}R_{88}+e_{22}R_{11}$ $+\frac{3}{2}e_{11}(R_{77}+R_{33})$	$[-3+$ $(\frac{1}{2}+i\kappa)P(e)]R_{23}$				$[-3+$ $(\frac{1}{2}+i\kappa)P(e)]R_{27}$	$[-(13/4)+2i\kappa P(e)]R_{28}$ $+\frac{3}{4}R_{82}$
2, 0		$[-3+$ $(\frac{1}{2}-i\kappa)P(e)]R_{32}$	$-3R_{33}+R_{77}$ $+e_{22}(\frac{1}{2}R_{88}+\frac{3}{2}R_{22})$ $+e_{11}(\frac{3}{2}R_{44}+\frac{1}{2}R_{66})$	$[-3+$ $(-\frac{1}{2}+i\kappa)P(e)]R_{34}$		$[-3+$ $(\frac{1}{2}-i\kappa)P(e)]R_{36}$	$-3R_{37}+R_{73}$	$[-3-$ $(\frac{1}{2}-i\kappa)P(e)]R_{38}$
2, −1			$[-3+$ $(-\frac{1}{2}-i\kappa)P(e)]R_{43}$	$[-(11/4)-P(e)]R_{44}$ $+\frac{3}{4}R_{66}+e_{11}R_{55}$ $+\frac{3}{2}e_{22}(R_{33}+R_{77})$	$[-\frac{5}{2}+$ $(-\frac{3}{2}+i\kappa)P(e)]R_{45}$	$[-(13/4)-2i\kappa P(e)]R_{46}$ $+\frac{3}{4}R_{64}$	$[-3-$ $(\frac{1}{2}+i\kappa)P(e)]R_{47}$	
2, −2				$[-\frac{5}{2}$ $(-\frac{3}{2}-i\kappa)P(e)]R_{54}$	$[-2-2P(e)]R_{55}$ $+e_{22}(3R_{66}+R_{44})$	$[-\frac{7}{2}-$ $(\frac{1}{2}+3i\kappa)P(e)]R_{56}$		
1, −1			$[-3+$ $(\frac{1}{2}+i\kappa)P(e)]R_{63}$	$[-(13/4)+2i\kappa P(e)]R_{64}$ $+\frac{3}{4}R_{46}$	$[-\frac{7}{2}-$ $(\frac{1}{2}-3i\kappa)P(e)]R_{65}$	$[-(11/4)+P(e)]R_{66}$ $+\frac{3}{4}R_{44}+3e_{11}R_{55}$ $+\frac{1}{2}e_{22}(R_{33}+R_{77})$	$[-3+$ $(\frac{1}{2}-i\kappa)P(e)]R_{67}$	
1, 0		$[-3+$ $(\frac{1}{2}-i\kappa)P(e)]R_{72}$	$-3R_{73}+R_{37}$	$[-3-$ $(\frac{1}{2}-i\kappa)P(e)]R_{74}$		$[-3+$ $(\frac{1}{2}+i\kappa)P(e)]R_{76}$	$-3R_{77}+R_{33}$ $+e_{22}(\frac{1}{2}R_{88}+\frac{3}{2}R_{22})$ $+e_{11}(\frac{3}{2}R_{44}+\frac{1}{2}R_{66})$	$[-3-$ $(\frac{1}{2}+i\kappa)P(e)]R_{78}$
1, 1	$[-\frac{7}{2}+$ $(\frac{1}{2}-3i\kappa)P(e)]R_{81}$	$[-(13/4)+2i\kappa P(e)]R_{82}$ $+\frac{3}{4}R_{28}$	$[-3-$ $(\frac{1}{2}+i\kappa)P(e)]R_{83}$				$[-3-$ $(\frac{1}{2}-i\kappa)P(e)]R_{87}$	$[-(11/4)-P(e)]R_{88}$ $+\frac{3}{4}R_{22}+3e_{22}R_{11}$ $+\frac{1}{2}e_{11}(R_{33}+R_{77})$

TABLE IX. The matrix $\boldsymbol{\sigma}(\mathrm{H})\cdot\boldsymbol{\sigma}(\overline{\mathrm{H}})$. The state labels are such that the first two numbers denote the state of one of the hydrogen atoms and the last two the state of the other hydrogen atom.

	1, 1; 1, 1	1, 0; 1, 1	1, −1; 1, 1	0, 0; 1, 1	1, 1; 1, 0	1, 0; 1, 0	1, −1; 1, 0	0, 0; 1, 0	1, 1; 1, −1	1, 0; 1, −1	1, −1; 1, −1	0, 0; 1, −1	1, 1; 0, 0	1, 0; 0, 0	1, −1; 0, 0	0, 0; 0, 0
1, 1; 1, 1	1															
1, 0; 1, 1				1	1								−1			
1, −1; 1, 1			−1			1		1						−1		−1
0, 0; 1, 0		1			−1								1			
1, 1; 1, 0		1		−1									1			
1, 0; 1,0			1					1								1
1, −1; 1, 0										1		1			−1	
0, 0; 1, 0			1					−						1		
1, 1; 1, −1						1	−1	−1						1		−1
1, 0; 1, −1							1					−1			1	
1, −1; 1, −1											1					
0, 0; 1, −1							1			−1					1	
1, 1; 0, 0		−1		1	1											
1, 0; 0, 0			−1				1	1								
1, −1; 0, 0						−1				1		1				
0, 0; 0, 0			−1			1		−1								

TABLE X. The expression for the change of the hydrogen density matrix due to spin-exchange collisions with other hydrogen atoms. When multiplied by $\frac{1}{4}V_{\mathrm{HH}}N_{\mathrm{H}}$ this matrix gives the time rate of change of the hydrogen density matrix due to spin-exchange collisions. The terms which average to zero have been neglected. This matrix summarizes 5 separate calculations and is valid only when one pair of off-diagonal matrix (e.g., H_{12} and H_{21}) is not equal to zero.

	1, 1	1, 0	1, −1	0, 0
1, 1	$\sigma_{SF}[(H_{22}+H_{44})^2-4H_{11}H_{33}-2H_{42}H_{24}]$ $+\sigma_{SF}'[(H_{22}-H_{44})^2+2H_{24}H_{42}]$	$\sigma_{SF}\{[-2+2(H_{11}-H_{33})]-2i\kappa(H_{33}-H_{22})\}H_{12}$ $+\sigma_{SF}'\{-2(H_{22}-H_{44})-2i\kappa'(H_{33}-H_{22})\}H_{12}$		$\sigma_{SF}\{-2+2(H_{11}-H_{33})-2i\kappa(H_{33}-H_{44})\}H_{14}$ $+\sigma_{SF}'\{2(H_{22}-H_{44})-2i\kappa'(H_{33}-H_{44})\}H_{14}$
1, 0	$\sigma_{SF}\{[-2+2(H_{11}-H_{33})]+2i\kappa(H_{33}-H_{22})\}H_{21}$ $+\sigma_{SF}'\{-2(H_{22}-H_{44})+2i\kappa'(H_{33}-H_{22})\}H_{21}$	$\sigma_{SF}\{-2(H_{22}-H_{44})-(H_{22}+H_{44})^2+4H_{11}H_{33}$ $-2H_{14}H_{41}-2H_{34}H_{43}+2H_{23}H_{32}$ $+2H_{12}H_{21}+2H_{42}H_{24}\}$ $+\sigma_{SF}'\{2(H_{22}-H_{44})-(5H_{22}+3H_{44})(H_{22}-H_{44})$ $-2H_{12}H_{21}-2H_{23}H_{32}-2H_{42}H_{24}$ $+2H_{14}H_{41}+2H_{34}H_{43}\}$	$\sigma_{SF}\{-2-2(H_{11}-H_{33})-2i\kappa(H_{22}-H_{11})\}H_{23}$ $+\sigma_{SF}'\{-2(H_{22}-H_{44})-2i\kappa'(H_{22}-H_{11})\}H_{23}$	$\sigma_{SF}\{-2-2i\kappa(H_{22}-H_{44})\}H_{24}$ $+\sigma_{SF}'\{2-4(H_{22}+H_{44})-2i\kappa'(H_{22}-H_{44})\}H_{24}$
1, −1		$\sigma_{SF}\{-2-2(H_{11}-H_{33})+2i\kappa(H_{22}-H_{11})\}H_{32}$ $+\sigma_{SF}'\{-2(H_{22}-H_{44})+2i\kappa'(H_{22}-H_{11})\}H_{32}$	$\sigma_{SF}\{(H_{22}+H_{44})^2-4H_{11}H_{33}-2H_{42}H_{24}\}$ $+\sigma_{SF}'\{(H_{22}-H_{44})^2+2H_{24}H_{42}\}$	$\sigma_{SF}\{-2-2(H_{11}-H_{33})-2i\kappa(H_{11}-H_{44})\}H_{34}$ $+\sigma_{SF}'\{2(H_{22}-H_{44})-2i\kappa'(H_{11}-H_{44})\}H_{34}$
0, 0	$\sigma_{SF}\{[-2+2(H_{11}-H_{33})+2i\kappa(H_{33}-H_{44})\}H_{41}$ $+\sigma_{SF}'\{2(H_{22}-H_{44})+2i\kappa'(H_{33}-H_{44})\}H_{41}$	$\sigma_{SF}\{-2+2i\kappa(H_{22}-H_{44})\}H_{42}$ $+\sigma_{SF}'\{2-4(H_{22}+H_{44})+2i\kappa'(H_{22}-H_{44})\}H_{42}$	$\sigma_{SF}\{-2-2(H_{11}-H_{33})+2i\kappa(H_{11}-H_{44})\}H_{43}$ $+\sigma_{SF}'\{2(H_{22}-H_{44})+2i\kappa'(H_{11}-H_{44})\}H_{43}$	$\sigma_{SF}\{2(H_{22}-H_{44})-(H_{22}+H_{44})^2+4H_{11}H_{33}$ $+2H_{14}H_{41}+2H_{34}H_{43}-2H_{23}H_{32}$ $-2H_{21}H_{12}+2H_{42}H_{24}\}$ $+\sigma_{SF}'\{-2(H_{22}-H_{44})+(5H_{44}+3H_{22})(H_{22}-H_{44})$ $+2H_{12}H_{21}+2H_{23}H_{32}-2H_{24}H_{42}$ $-2H_{14}H_{41}-2H_{34}H_{43}\}$

will be shifted in the same direction and that the linewidth of the $\Delta m=\pm 1$ transitions will depend upon the electron polarization.

A second system of interest is rubidium colliding with electrons where there are off-diagonal elements of the rubidium density matrix. We will make the calculations for Rb^{87} and we will assume that the electron density matrix has no off-diagonal elements. We will use e_{ij} to denote the elements of the electron density matrix, R_{ij} to denote the elements of the rubidium density matrix, and $P(e)$ to denote the electron polarization. For the rubidium density matrix the indices 1 through 8 denote the states (2,2), (2,1), (2,0), (2, −1), (2, −2), (1, −1), (1,0), and (1,1), respectively. The matrix for $\boldsymbol{\sigma}(Rb^{87})\cdot\boldsymbol{\sigma}(e)$ is summarized in Table IV. The change in the rubidium density matrix due to spin-exchange collisions can be calculated from Eq. (27). The result of this calculation is summarized in Table VIII. As written this matrix is the summary of 15 independent calculations and it is only valid when one pair of off-diagonal matrix elements such as R_{21} and R_{12} are present. This result is very similar to that obtained for the hydrogen-electron system and the same kind of observations can be made about it.

A third system of interest is that of hydrogen atoms colliding with hydrogen atoms. For this situation the two particles are identical and the calculation must be modified to take this into account. This can be done by using the expression

$$\rho=\tfrac{1}{2}\textstyle\sum_k[|k\rangle|s\rangle+|-k\rangle Q|s\rangle]\times P(k,s)[\langle s|\langle k|+\langle s|Q\langle -k|], \quad \text{(B1)}$$

for the initial density matrix. Here Q is the operator which interchanges the two hydrogen atoms (both proton and electrons) and the wave functions have been normalized so that there are two particles in the box. The equation for the change of the density matrix [Eq. (27)] then becomes

$$\begin{aligned}\frac{d\rho(\mathrm{H})}{dt}=&\frac{v_{\mathrm{HH}}N_{\mathrm{H}}}{4}\{\sigma_{\mathrm{SF}}\,\mathrm{Tr}_{\mathrm{H}}[-3\rho(\mathrm{H},\bar{\mathrm{H}})\\&+(1+2i\kappa)(\sigma(\mathrm{H})\cdot\sigma(\bar{\mathrm{H}}))\rho(\mathrm{H},\bar{\mathrm{H}})\\&+(1-2i\kappa)\rho(\mathrm{H},\bar{\mathrm{H}})(\sigma(\mathrm{H})\cdot\sigma(\bar{\mathrm{H}}))\\&+(\sigma(\mathrm{H})\cdot\sigma(\bar{\mathrm{H}}))\rho(\mathrm{H},\bar{\mathrm{H}})(\sigma(\mathrm{H})\cdot\sigma(\bar{\mathrm{H}}))]\\&+\sigma_{\mathrm{SF}'}\,\mathrm{Tr}_{\mathrm{H}}[-3\rho(\mathrm{H},\bar{\mathrm{H}})Q\\&+(1+2i\kappa')(\sigma(\mathrm{H})\cdot\sigma(\bar{\mathrm{H}}))Q\rho(\mathrm{H},\bar{\mathrm{H}})\\&+(1-2i\kappa')\rho(\mathrm{H},\bar{\mathrm{H}})Q(\sigma(\mathrm{H})\cdot\sigma(\bar{\mathrm{H}}))\\&+(\sigma(\mathrm{H})\cdot\sigma(\bar{\mathrm{H}}))Q\rho(\mathrm{H},\bar{\mathrm{H}})(\sigma(\mathrm{H})\cdot\sigma(\bar{\mathrm{H}}))]\}, \quad \text{(B2)}\end{aligned}$$

where

$$\sigma_{\mathrm{SF}}=\frac{\pi}{k^2}\sum_{l=0}^{\infty}(2l+1)\sin^2(\delta_l{}^3-\delta_l{}^1), \quad \text{(B3)}$$

$$\sigma_{\mathrm{SF}\kappa}=\frac{\pi}{2k^2}\sum_{l=0}^{\infty}(2l+1)\sin 2(\delta_l{}^3-\delta_l{}^1), \quad \text{(B4)}$$

$$\sigma_{\mathrm{SF}'}=\frac{\pi}{k^2}\sum_{l=0}^{\infty}(2l+1)(-1)^l\sin^2(\delta_l{}^3-\delta_l{}^1), \quad \text{(B5)}$$

$$\sigma_{\mathrm{SF}'\kappa'}=\frac{\pi}{2k^2}\sum_{l=0}^{\infty}(2l+1)(-1)^l\sin 2(\delta_l{}^3-\delta_l{}^1). \quad \text{(B6)}$$

The matrix for $\sigma(\mathrm{H})\cdot\sigma(\bar{\mathrm{H}})$ is summarized in Table IX. The expression for the time rate of change of the hydrogen density matrix is summarized in Table X.